AD-A191 848 A METHOD FOR DISCRIMINATION OF RADAR TARGETS USING COMPLEX NATURAL RESONANCES(U) OHIO STATE UNIV COLUMBUS ELECTROSCIENCE LAB E P BOHLEY SEP 87 ESL-718048-4 1/1

UNCLASSIFIED N00014-86-K-0202 F/G 17/9 NL

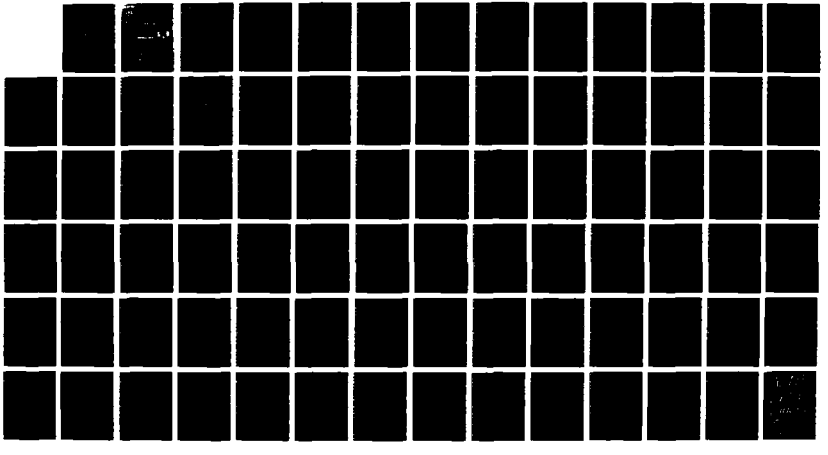

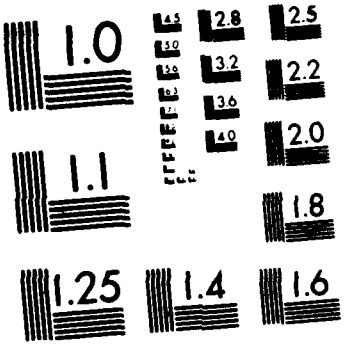

A METHOD FOR DISCRIMINATION OF RADAR TARGETS USING COMPLEX NATURAL RESONANCES

Eric P. Bohley

The Ohio State University

ElectroScience Laboratory

Department of Electrical Engineering
Columbus, Ohio 43212

Technical Report No. 718048-4
Contract No. N00014-86-K-0202
September 1987

Department of the Navy
Office of Naval Research
800 North Quincy Street
Arlington, Virginia 22217-5000

50272-101

REPORT DOCUMENTATION PAGE	1. REPORT NO.	2.	3. Recipient's Accession No.

4. Title and Subtitle

A METHOD FOR DISCRIMINATION OF RADAR TARGETS USING COMPLEX NATURAL RESONANCES

5. Report Date September 1987

6.

7. Author(s)

Eric P. Bohley

8. Performing Organization Rept. No. 718048-4

9. Performing Organization Name and Address

The Ohic State University
ElectroScience Laboratory
1320 Kinnear Road
Columbus, Ohio 43212

10. Project/Task/Work Unit No.

11. Contract(C) or Grant(G) No.

(C) N00014-86-K-0202

(G)

12. Sponsoring Organization Name and Address

Department of the Navy
Office of Naval Research
800 North Quincy Street
Arlington, Virginia 22217-5000

13. Type of Report & Period Covered Technical Report

14.

15. Supplementary Notes

16. Abstract (Limit: 200 words)

A prediction-correlation target discrimination algorithm using target complex natural resonances is investigated. The targets natural resonances are extracted from experimentally measured frequency domain scattering data. Scattering data were obtained from scale model targets measured in the ElectroScience Laboratory compact radar range facility. The targets used are models of three military ground vehicles.

Signal processing required for the extraction of poles is described. The principles of the prediction-correlation algorithm are discussed and the algorithm is demonstrated for both noiseless data and data with additive white noise. Classification results are plotted for the targets at aspect angles of 0, 10, 20, 30, 60, and 90 degrees from nose on.

17. Document Analysis a. Descriptors

b. Identifiers/Open-Ended Terms

c. COSATI Field/Group

18. Availability Statement

APPROVED FOR PUBLIC RELEASE
DISTRIBUTION IS UNLIMITED

19. Security Class (This Report) Unclassified

20. Security Class (This Page) Unclassified

21. No. of Pages 73

22. Price

(See ANSI-Z39.18) See Instructions on Reverse OPTIONAL FORM 272 (4-77) (Formerly NTIS-35) Department of Commerce

TABLE OF CONTENTS

LIST OF TABLES

LIST OF FIGURES

FIGURE PAGE

CHAPTER I

INTRODUCTION

The capability of classifying or identifying radar targets from their scattering characteristics is of considerable interest to designers of future radar systems. Target classification falls into two two basic categories; discrimination, where a priori knowledge of the class of targets and certain target features are available, and target identification, where little or no a priori knowledge of the target(s) is available. The technique described in this report is a discrimination technique involving a *library of information* about expected targets. The features utilized are the dominant or near dominant complex natural resonances (CNR's) of the target as well as certain aspect-dependent information. Various discrimination techniques employing CNR's have been developed in [2,14,16,20], the technique used in this work involves the reconstruction of a target response using previously extracted CNR's.

The interaction of a target with an electromagnetic wave is best summarized by its canonical waveforms, i.e., impulse, step, and ramp responses. The possibility of approximating the transfer function of a distributed parameter system at sufficiently low frequencies by a lumped

parameter linear model was first suggested by Kennaugh and Cosgriff [5] and later formalized by Kennaugh and Moffatt [6]. The fact that the response is dominated by a few dominant complex natural resonances in the low resonance region led to the rational function concept of approximating the frequency domain response. In [6] C.E. Baum developed a mathematical model called "the singularity expansion method" , which suggests the existence of complex natural resonances when an electromagnetic wave excites any perfectly conducting body. Theoretical methods have been developed for calculating the complex natural resonances of certain simple geometries. These geometries include dielectric spheres [7], conducting spheres [8] and thin prolate spheroids [9]. When the vector wave equation is separable (sphere and thin circular disk) transcendental equations can be obtained (only for the sphere to date) for the CNR's. For other geometries, an integral equation formulation and numerical search can be used for electrically small objects. For the general target, the CNR's must be extracted from measured scattering or radiation data. Various methods for extracting resonances using rational functions are given in [10] and [12].

There has been some controversy over the need for inclusion of an entire function to completly model the scattering transfer function [4]. The situation seems best summarized by Felson [11] and the need for an entire function is now generally accepted. The distinction between free and forced response, and correspondingly the rational and entire function part of the representation, is best illustrated for the case of

an aperiodic illumination of a simple object, such as a sphere. In this case, the initial response is a forced response as the wavefront moves over the sphere. After a time corresponding to two sphere diameters the received response is purely free response as the wavefront moves beyond the sphere. The situation is much more complex when a complicated target is illuminated. Here individual substructures of the target may be resonating well before the wavefront moves beyond the target. Waiting until the wavefront has moved beyond the target ensures a purely free response but resonances that have decayed to inextractable levels are likely to be missed. It should be kept in mind that the entire function is essentially a high frequency contribution, as pointed out by Felson [11]. The ability to extract poles and their usefullness in discrimination will also have a high frequency limit because as frequency is increased the density of poles will preclude extraction.

In theory the CNR'sof a target are excitation invariant. In practice however we find that the real part of the CNR's are not excitation invariant at some aspect angles. At certain aspect angles some pole combinations will not be excited or only weakly excited. Thus some poles may not appear at certain aspect angles and the real part of the poles can be expected to change significantly. A target must therefore be considered as several targets depending on aspect angle and polarization.

The targets utilized in this work are scale models of three military ground vehicles whose radar cross sections were measured on the

Ohio State University Electroscience Laboratory compact radar range. Measurement, preprocessing and pole extraction are discussed in Chapter II. In Chapter III the discrimination algorithm is formulated and applied at several aspect angles for both noisy and noise-free cases. Chapter III contains a summary, conclusions and recommendations for further research.

CHAPTER II

EXTRACTION OF COMPLEX NATURAL RESONANCES

The problem of approximating any transient function by a finite sum of weighted exponentials was first solved by Prony in 1795 [13], leading to the concept of CNR's. Since that time various methods have been developed for extracting CNR's in both the time and frequency domain [10,12,14]. The method used in this work is a frequency domain extraction technique based on a rational function fit. The first section of this chapter describes the preprocessing steps necessary in order to extract Complex Natural Resonances (CNR)'s from measured frequency domain complex scattering data. The theoretical details of the rational function method are presented in the third and fourth sections of this chapter. The last two sections of this chapter present the results of applying the described techniques to measured data and an indication of the stability that can be expected in the extracted poles of a target as a function of aspect angle.

A. PREPROCESSING OF DATA FOR POLE EXTRACTION

Broadband backscatter measurements of the targets considered were obtained on the Ohio State University Electroscience Laboratory compact range. Proper preprocessing is essential to obtain valid results in pole extraction and target discrimination.

The first preprocessing step is the calibration of the raw data measured on the range. Calibration involves the subtraction of background and clutter and normalization with respect to a sphere. At each measured data point the calibration equation is

$$\tilde{T}_i^c = \tilde{E}_i^s \frac{\tilde{T}_i - \tilde{B}_i^T}{\tilde{S}_i - \tilde{B}_i^s} \tag{2.1}$$

where "~" refers to the complex representation of the amplitude and phase at the i^{th} data point. The subscript i refers to the frequency corresponding to a data point through the following relation

$$X_i = X(\omega_o + (i-1)\Delta\omega) \tag{2.2}$$

where (ω_o) and $(\Delta\omega)$ are the initial and increment frequencies. The following terminology is adopted in Equation (2.1).

$\tilde{T}^c$ is the calibrated data,

$\tilde{T}$ is the target raw data,

$\tilde{B}^T$ is the target background data,

$\tilde{S}$ is the sphere raw data,

$\tilde{B}^s$ is the sphere background data, and

$\tilde{E}^s$ is the exact (calculated) sphere data.

More detailed discussions of range measurement and calibration procedures are available in [1] and [15].

Measurement of targets on a ground plane introduces problems which are not present in the measurement of targets on low RCS mounts. Ground plane edge diffraction effects are chief among these problems. When targets are mounted on or removed from ground planes slight positional offsets may occur (usually on the order of half a millimeter) which result in incomplete cancellation of ground plane edge diffraction terms (see Figure 2.1).

Note that the time response in all time domain plots correspond to a two way path length for the radar incident wave. Time domain plots were produced by applying an Inverse Fourier transform to calibrated frequency data measured in the 2 to 18 GHz frequency range. To reduce Gibb's phenomena caused by truncation of the data outside the 2 to 18 GHz range the frequency domain data was first windowed with a Kaiser-Bessel band pass window.

Targets were measured on a circular ground plane of 104 centimeters (cm.) diameter at an elevation angle of 30 degrees (see Figure 2.2). The targets had lengths ranging from about 6 to 8 (cm.), and were placed at the center of the ground plane. The path length from the leading edge of a ground plane to the leading edge of a ground vehicle is 48 cm. and 41.6 cm from the ground vehicles leading edge plane, which is perpendicular to the incident radar ray, (see Figure 2.2). Thus the first ground plane edge to ground vehicle interaction term will occur approximately 3 nanoseconds (ns) after the ground plane leading edge diffraction term. This term is thus embedded in the target response and not removable.

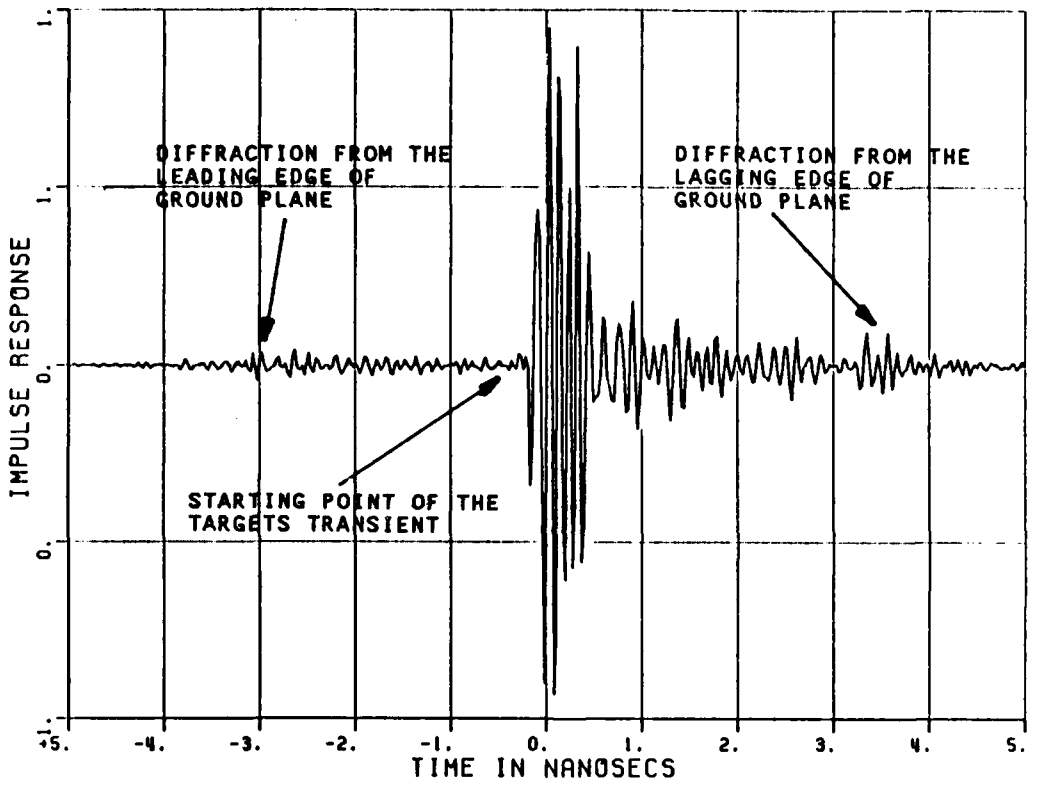

Figure 2.1. The impulse response of ground vehicle T1 at 0 degrees, obtained from Fourier transformation of bandlimited spectral data (2-18) GHz).

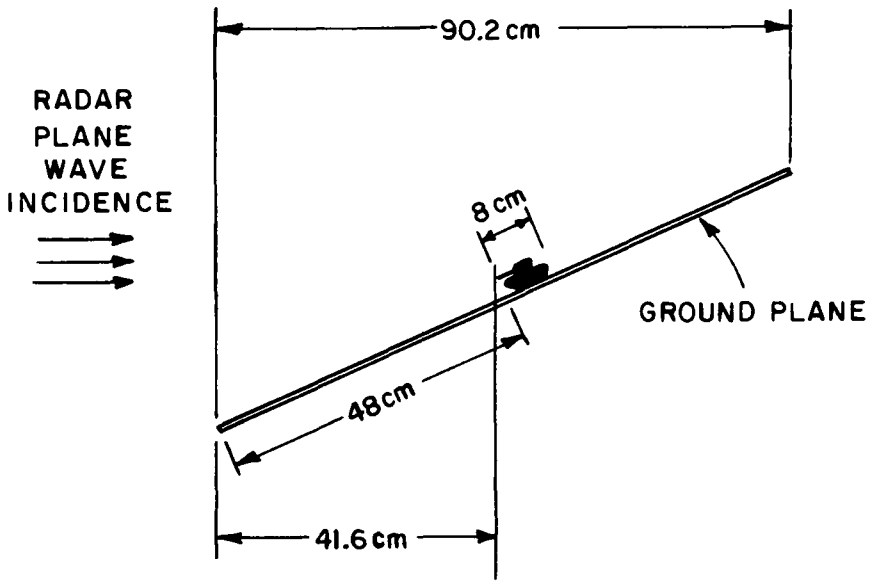

Figure 2.2. The ground plane-ground vehicle configuration. The ground plane is flat and circular.

Ground plane edge effects which are separate from the target response (see Figure 2.3) and other clutter not removed during calibration is removed using a tenth order Butterworth digital filter. A Fortran program originally written by T. Lee [10] and later modified by C.Y. Lai* is used for this task. The program operates on frequency domain data and corresponds to a tenth order Butterworth time domain window. Further details are available in [10] and [18].

The results of filtering can be seen in Figures 2.3 to 2.6. In Figures 2.1 and 2.3 the target's transient response has decayed almost down to the background level before the time of occurrence of the ground plane trailing edge transient. Thus we conclude that the elimination of the response beyond this point is not very critical.

B. THEORETICAL FORMULATION

A radar scatterer has an infinite number of CNR's and is therefore a system of infinite order. The response of a target to an impulse, or in fact any aperiodic illumination consists of two parts. First is a forced response as the wavefront moves across the target. Second is a free or natural response as the wavefront moves beyond the target. In the s domain the transfer function of the target can be modelled as a residue series plus an entire function [22].

$$F(s) = \sum_{n=1}^{\infty} \frac{R_n(\Omega)}{s-s_n} + G(s,\Omega) \quad , \tag{2.3}$$

* ElectroScience Laboratory

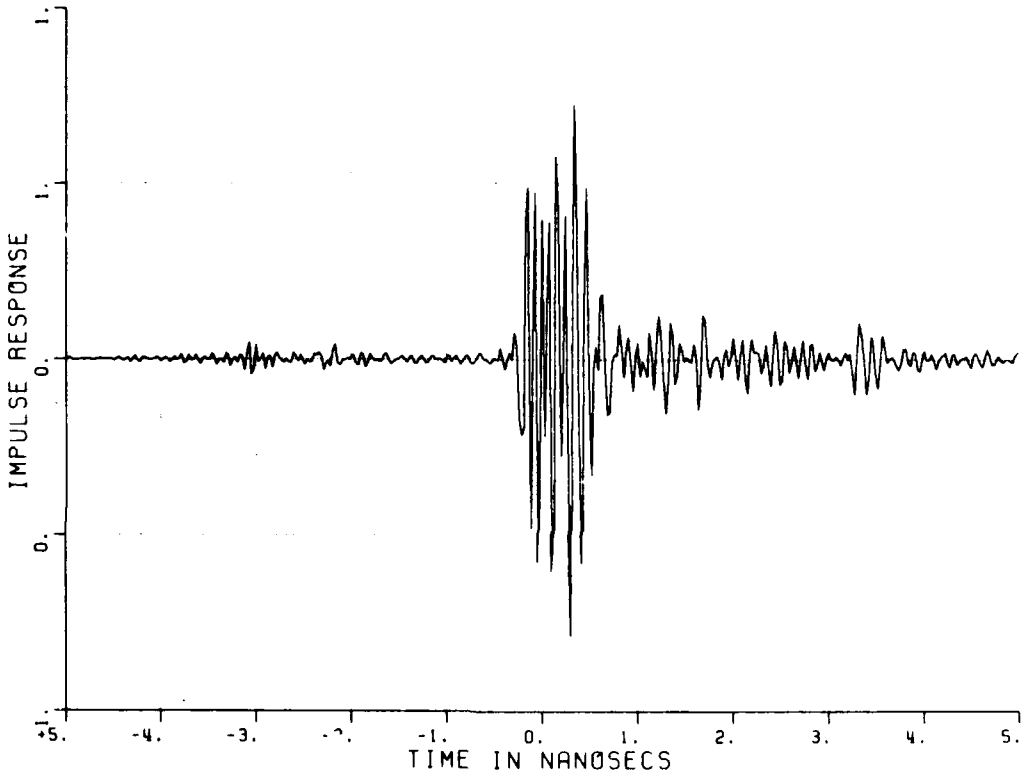

Figure 2.3. The impulse response of ground vehicle T1 at 0 degrees, obtained via Fourier transformation of measured and calibrated frequency domain data (2 to 18 GHz). Vertical polarization.

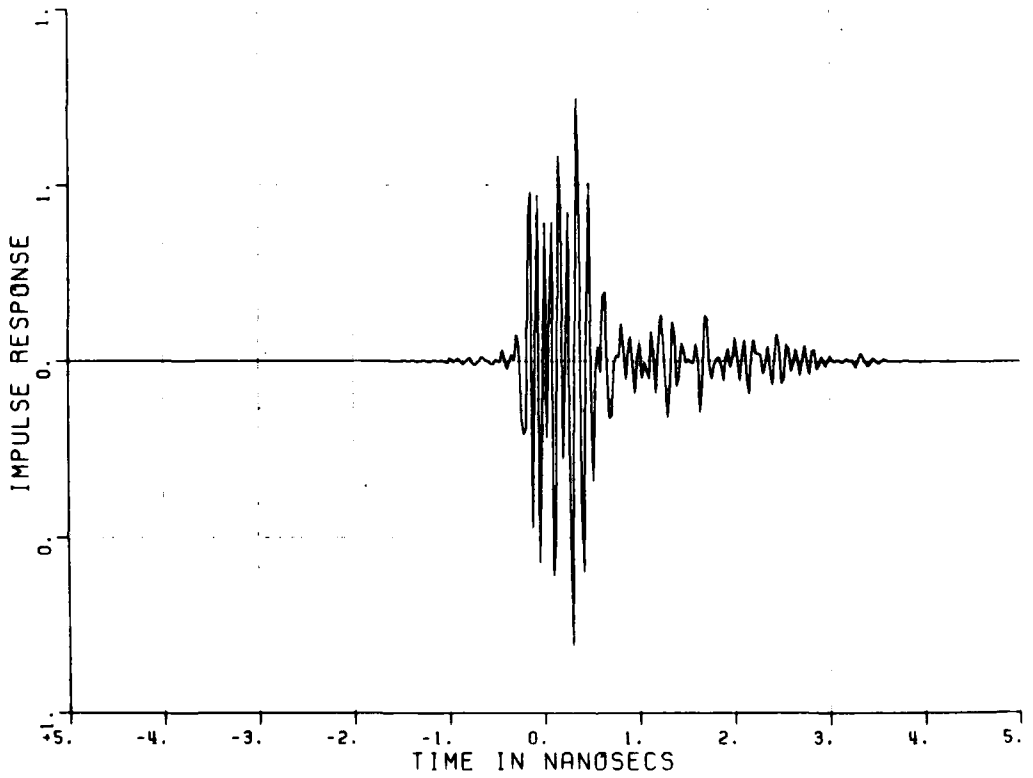

Figure 2.4. The impulse response of ground vehicle T1 at 0 degrees, obtained via Fourier transformation of the digitally filtered data. Note that the edge diffractions are significantly reduced. Vertical polarization. The equivalent time window of the digital filter is -1.0 to +3.0 ns.

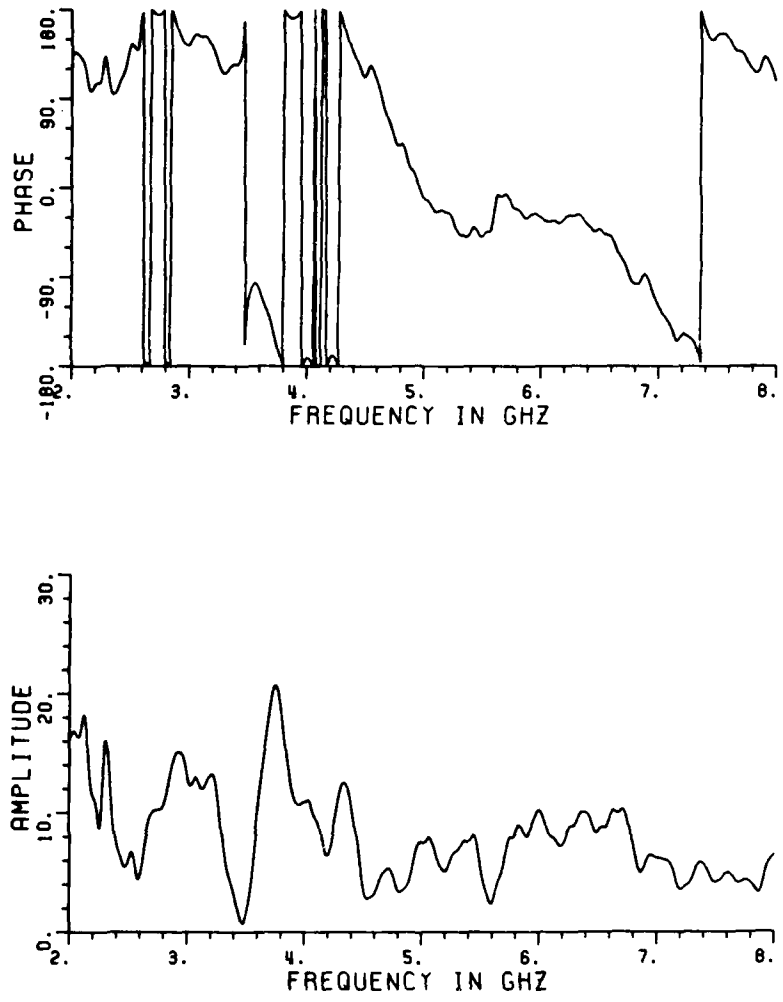

Figure 2.5. Plots of calibrated unfiltered spectral data (amplitude and phase), for ground vehicle T1 at an aspect angle of 0 degrees, using vertical polarizaiton.

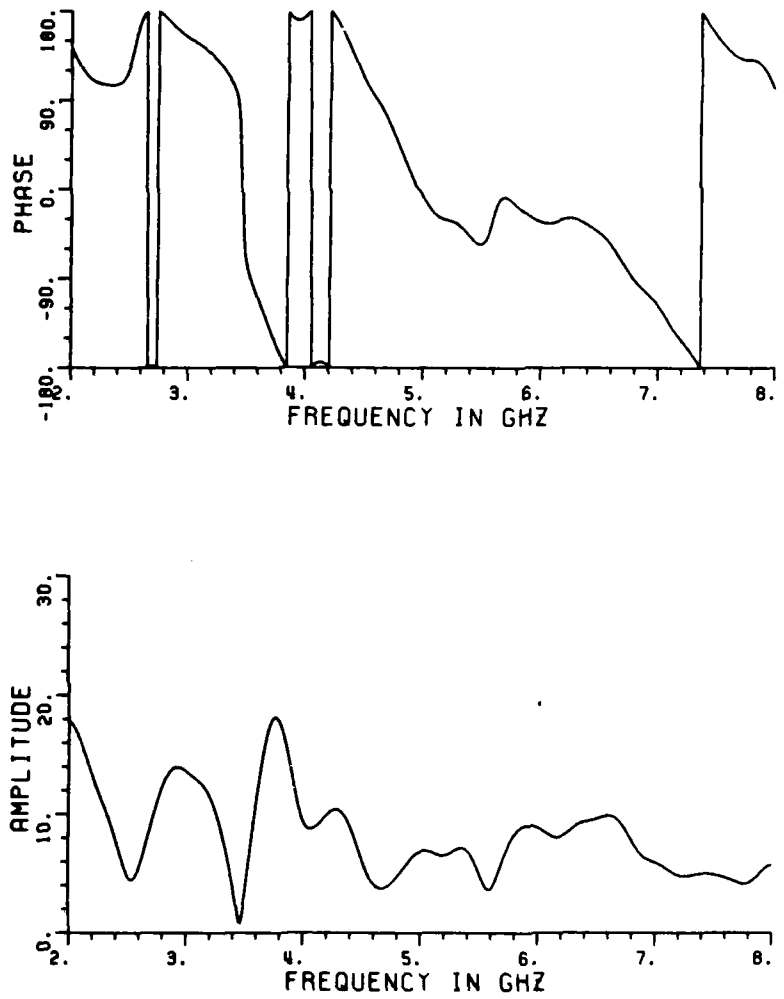

Figure 2.6. Plots of calibrated digitally filtered spectral data (amplitude and phase). The data is smoothed using an equivalent time window from -1.0 to +3.0 ns. Vertical polarization at an aspect angle of 0 degrees.

where the R_n are aspect (Ω) dependent residues, s_n are the the natural resonances and $G(s,\Omega)$ is an entire function. An entire function is a function that is analytic at each point in the entire plane. Note that the entire function is dependent on both aspect and frequency.

Since we are interested in the transfer function over a limited bandwidth only a limited number of CNR's will contribute significantly. Thus the response to an impulse input is actually of the form

$$Y(s) = \sum_{n=1}^{N} \frac{R_n}{s-s_n} + \hat{G}(s,\Omega) + N_{(s)} \quad , \tag{2.4}$$

$$\text{where } \hat{G}(s,\omega) = \begin{cases} G(s,\Omega) & \text{within the passband} \\ 0 & \text{outside the passband} \end{cases}$$

and $N(s)$ is the noise present in any practical measurement. The methods used to remove, as much as possible, the noise from the measured spectrum, were discussed in the previous section.

There is, at present, no way to determine the entire function part of the response for a complicated target. In this work a simple attempt is made to approximate the entire function by constant a plus another constant b times s as suggested by Lai and Moffatt [22]. This corresponds to an impulse and a doublet in time domain. This choice is motivated by the fact that the impulse response of several simple objects have impulse or doublet singularities. The rational function is then written as

$$F(s) = \frac{b_0 + b_1 s + b_2 s^2 + \ldots + b_{N+1} s^{N+1}}{1 + a_1 s + a_2 s^2 + \ldots + a_N s^N} \qquad (2.5)$$

For real frequency data, s is replaced by jw. The CNR's are found by finding the roots of the polynomial in the denominator of Equation (2.5).

Since the system is real, the poles should appear in complex conjugate pairs in the LHP. The coefficients of the denominator should therefore be real and positive. The coefficients can be forced to be real by separating Equation (2.5) into real and imaginary parts [22]. This has the added advantage that negative frequency data are not required. Unfortunately this procedure does not guarantee all the coefficients to be positive, thus some of the extracted poles may appear in the RHP.

The parameter N in Equation (2.5) is the number of poles requested. Since the number of poles in a given frequency range is not known a priori, several different system orders are tried for each range. The number of data points used should be close to or equal to twice the number of poles requested. This will result in an overdetermined system of linear equations. A Chebeychev solution is employed in order to minimize the peak error as opposed to the mean squared error. Thus the maximum element of the residual vector [b-Ax] is minimized in solving for x in Ax=b. For this task, an efficient program [21] using the simplex method is employed.

Poles are extracted in overlaping frequency intervals of approximately 1.0 to 1.5 GHz bandwidth. Searching overlaping frequency

intervals helps to eliminate curve fitting poles. In each interval searched the system order and sample points are varied over a range of values. There are few values of N and sampling at which the LHP poles are stable and within the range of frequency searched. The best results are obtained by choosing the endpoints of the frequency range searched at or near minima.

C. CALCULATING THE CORRESPONDING RESIDUES

After solving for the system poles the next step is to use the chosen LHP poles to fit the spectrum and solve for their corresponding residues. Rewriting Equation (2.5)

$$F(s) = \sum_{n=1}^{N} \frac{R_n}{s-p_n} + a + bs \qquad (2.6)$$

where

N is the number of LHP poles,

p_n are the extracted LHP poles,

R_n is the residue of pole p_n,

a,b are unknown real constants.

The Chebeychev norm is again used in solving the system of equations. Negative frequency information must be used so that the residues of every pole pair are complex conjugates.

D. THE RESULTS OF POLE EXTRACTION

The targets utilized in this work were three military ground vehicles designated "T1", "T3", and "A1". As previously described the targets were measured on a ground plane at an elevation angle of 30 degrees using vertical polarization. Targets are measured at various aspect angles and a frequency file created for each aspect angle. Aspect angles of 0, 10, 20, 30, 60, and 90 degrees from head on were chosen for pole extraction. After the appropriate preprocessing poles are extracted for each target at each aspect angle. The results of pole extraction are given in Tables 2.1 to 2.6.

A target spectrum may be reconstructed over a finite bandwidth using a pole set and a set of optimized parameters. The parameters are a starting, middle, and ending frequency along with a set of sampling points chosen to provide the best fit (in a mean-square error sense) to the original spectrum. The method of reconstruction and the selection of optimal parameters are discussed in Chapter III. Plots of measured and predicted spectra at selected aspect angles are shown in Figures 2.7 to 2.10. The discontinuity near the center of the frequency band is due to the fact that the frequency range is divided into two intervals and each is approximated by a separate function. The reason for separation is that the approximation deteriorates if an attempt is made to apply it over a range of more than about 1.5 GHz (model scale frequency) using more than six or seven pole pairs.

TABLE 2.1

LIST OF POLE SETS FOR GROUND VEHICLE "T1" AT ASPECT ANGLES OF 0, 10 AND 20, FOR LINEAR VERTICAL POLARIZATION (OSCILLATORY PARTS IN GHz; REAL PARTS IN 10^9 NEPERS/s)

0 DEGREES		10 DEGREES		20 DEGREES	
REAL	IMAGINARY	REAL	IMAGINARY	REAL	IMAGINARY
-.234	2.77	-.249	2.86	-.181	2.75
-.138	3.39	-.191	3.63	-.339	3.14
-.196	3.55	-.202	4.05	-.193	3.44
-.120	3.76	-.249	4.43	-.088	3.76
-.199	3.82	-.266	4.81	-.114	4.34
-.248	4.44	-.199	5.03	-.236	4.99
-.208	4.77	-.154	5.43	-.113	5.39
-.189	5.53	-.203	5.74	-.072	5.51
-.321	5.90	-.073	6.34	-.045	6.19
-.088	6.70	-.122	6.65	-.178	6.73
-.760	6.87			-.317	7.57

TABLE 2.2

LIST OF POLE SETS FOR GROUND VEHICLE "T1" AT ASPECT ANGLES OF 30, 60 AND 90, FOR LINEAR VERTICAL POLARIZATION (OSCILLATORY PARTS IN GHz; REAL PARTS IN 10^9 NEPERS/s)

30 DEGREES		60 DEGREES		90 DEGREES	
REAL	IMAGINARY	REAL	IMAGINARY	REAL	IMAGINARY
-.181	2.75	-.262	2.63	-.146	2.76
-.339	3.14	-.553	3.08	-.147	3.57
-.193	3.44	-.184	3.23	-.057	3.90
-.088	3.76	-.167	3.56	-.389	4.34
-.114	4.34	-.144	3.88	-.360	4.91
-.236	4.99	-.392	4.57	-.175	5.74
-.113	5.39	-.391	5.16	-.099	6.28
-.072	5.51	-.238	5.42	-.214	6.79
-.045	6.19	-.185	6.14	-.114	7.73
-.178	6.73	-.125	6.66		
-.317	7.57	-.146	7.32		

TABLE 2.3

LIST OF POLE SETS FOR GROUND VEHICLE "T3" AT ASPECT ANGLES OF 0, 10 AND 20, FOR LINEAR VERTICAL POLARIZATION (OSCILLATORY PARTS IN GHz; REAL PARTS IN 10^9 NEPERS/s)

0 DEGREES		10 DEGREES		20 DEGREES	
REAL	IMAGINARY	REAL	IMAGINARY	REAL	IMAGINARY
-.253	2.25	-.176	2.28	-.153	2.48
-.142	2.82	-.112	2.76	-.258	3.05
-.259	2.97	-.211	3.00	-.369	3.19
-.258	3.24	-.196	3.31	-.469	3.78
-.173	3.57	-.189	3.73	-.145	4.10
-.183	3.82	-.139	4.35	-.318	4.37
-.159	4.39	-.179	4.72	-.141	4.93
-.274	4.68	-.338	4.99	-.117	5.66
-.322	5.05	-.308	5.42	-.146	6.28
-.276	5.64	-.432	5.53	-.133	7.00
-.118	6.01	-.343	5.81		
-.681	6.44	-.191	6.27		
-.248	6.88	-.204	6.94		

TABLE 2.4

LIST OF POLE SETS FOR GROUND VEHICLE "T3" AT ASPECT ANGLES OF 30, 60 AND 90, FOR LINEAR VERTICAL POLARIZATION (OSCILLATORY PARTS IN GHz; REAL PARTS IN 10^9 NEPERS/s)

30 DEGREES		60 DEGREES		90 DEGREES	
REAL	IMAGINARY	REAL	IMAGINARY	REAL	IMAGINARY
-.409	2.24	-.238	2.53	-.189	2.39
-.213	2.98	-.082	2.75	-.154	2.78
-.285	3.28	-.149	3.17	-.073	3.25
-.326	3.84	-.136	3.98	-.258	3.79
-.093	4.32	-.237	4.19	-.159	4.08
-.248	4.70	-.197	4.45	-.196	4.67
-.135	5.22	-.157	4.77	-.128	5.31
-.107	5.48	-.082	4.98	-.089	6.07
-.238	6.15	-.095	5.51	-.302	6.75
-.127	6.78	-.382	6.03		
		-.126	6.64		
		-.097	7.40		

TABLE 2.5

LIST OF POLE SETS FOR GROUND VEHICLE "A1" AT ASPECT ANGLES OF 0, 10 AND 20, FOR LINEAR VERTICAL POLARIZATION (OSCILLATORY PARTS IN GHz; REAL PARTS IN 10^9 NEPERS/s)

0 DEGREES		10 DEGREES		20 DEGREES	
REAL	IMAGINARY	REAL	IMAGINARY	REAL	IMAGINARY
-.327	2.61	-.169	2.89	-.097	2.79
-.134	3.00	-.149	3.42	-.347	3.06
-.153	3.62	-.189	3.95	-.191	3.34
-.430	4.04	-.091	4.49	-.229	3.92
-.036	4.32	-.080	5.06	-.179	4.26
-.079	5.00	-.882	5.85	-.127	4.76
-.245	5.79	-.124	6.38	-.345	5.60
-.508	5.99	-.169	6.69	-.316	5.89
-.107	6.28	-.256	7.40	-.109	6.26
-.189	6.57			-.164	6.75
-.094	7.13				

TABLE 2.6

LIST OF POLE SETS FOR GROUND VEHICLE "A1" AT ASPECT ANGLES OF 30, 60 AND 90, FOR LINEAR VERTICAL POLARIZATION (OSCILLATORY PARTS IN GHz; REAL PARTS IN 10^9 NEPERS/s)

30 DEGREES		60 DEGREES		90 DEGREES	
REAL	IMAGINARY	REAL	IMAGINARY	REAL	IMAGINARY
-.177	2.94	-.129	2.46	-.247	2.09
-.151	3.36	-.125	2.86	-.061	2.84
-.239	4.00	-.023	3.07	-.112	3.34
-.215	4.47	-.162	3.33	-.133	3.64
-.131	4.92	-.193	3.64	-.105	4.04
-.007	5.27	-.176	4.35	-.119	4.50
-.121	6.04	-.242	4.71	-.211	4.84
-.229	6.12	-.126	5.21	-.225	5.08
-.096	6.29	-.795	5.93	-.332	5.81
-.189	6.72	-.224	6.24	-.131	6.37
-.341	7.36	-.138	6.59	-.209	6.79
		-.135	7.39		

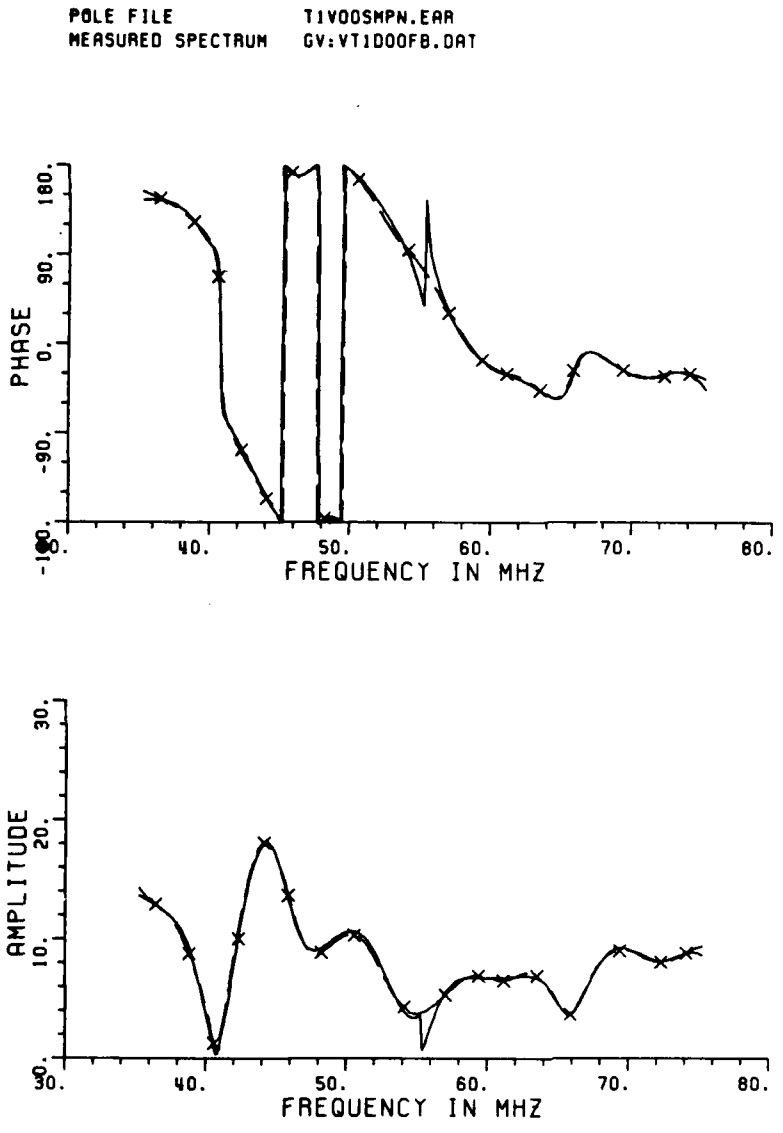

Figure 2.7. Amplitude and phase plots vs. frequency of original (dashed) and predicted (solid) spectra for ground vehicle "T1" at an aspect angle of 0 degrees, using linear polarization.

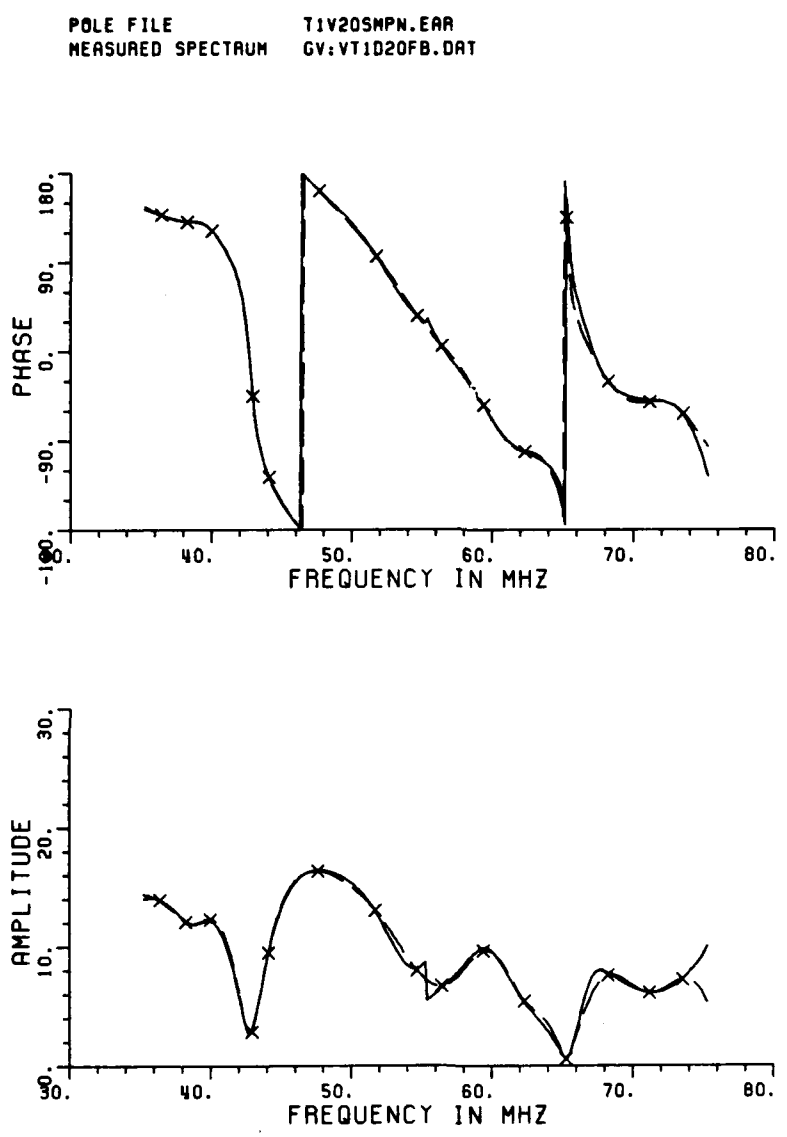

Figure 2.8. Amplitude and phase plots vs. frequency of original (dashed) and predicted (solid) spectra, for ground vehicle "T1" at an aspect angle of 20 degrees, using linear polarization.

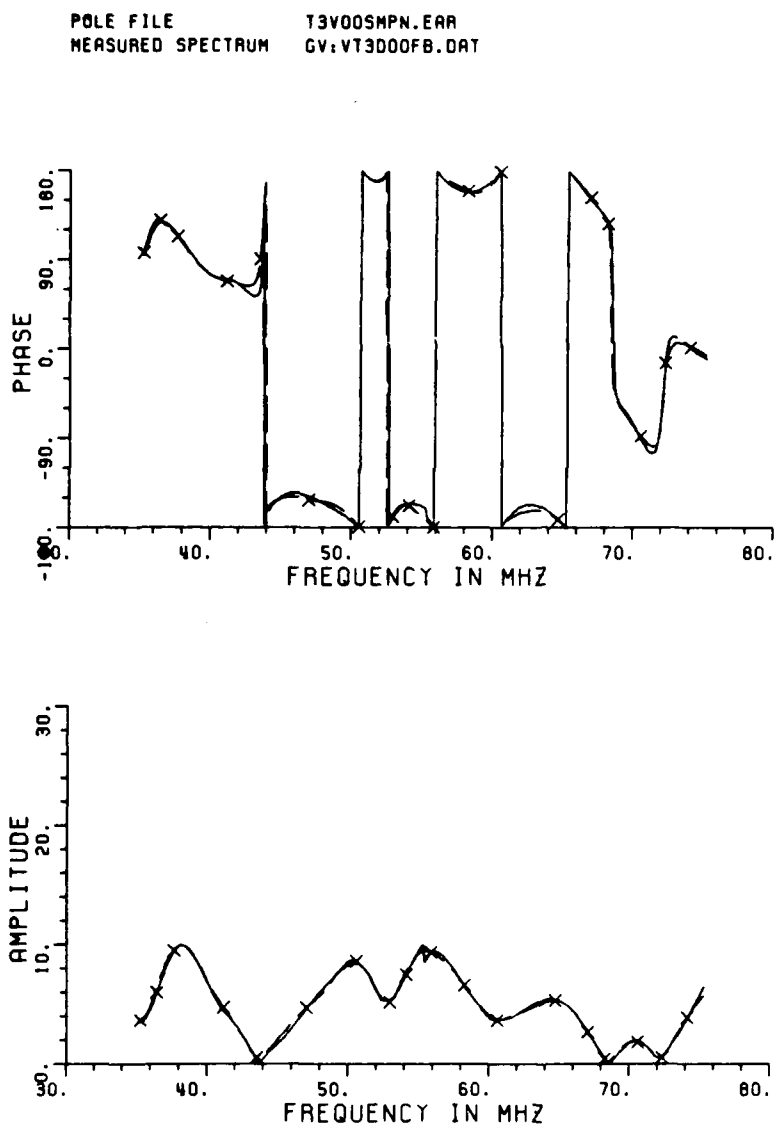

Figure 2.9. Amplitude and phase plots vs. frequency of original (dashed) and predicted (solid) spectra, for ground vehicle "T3" at an aspect angle of 0 degrees, using linear polarization.

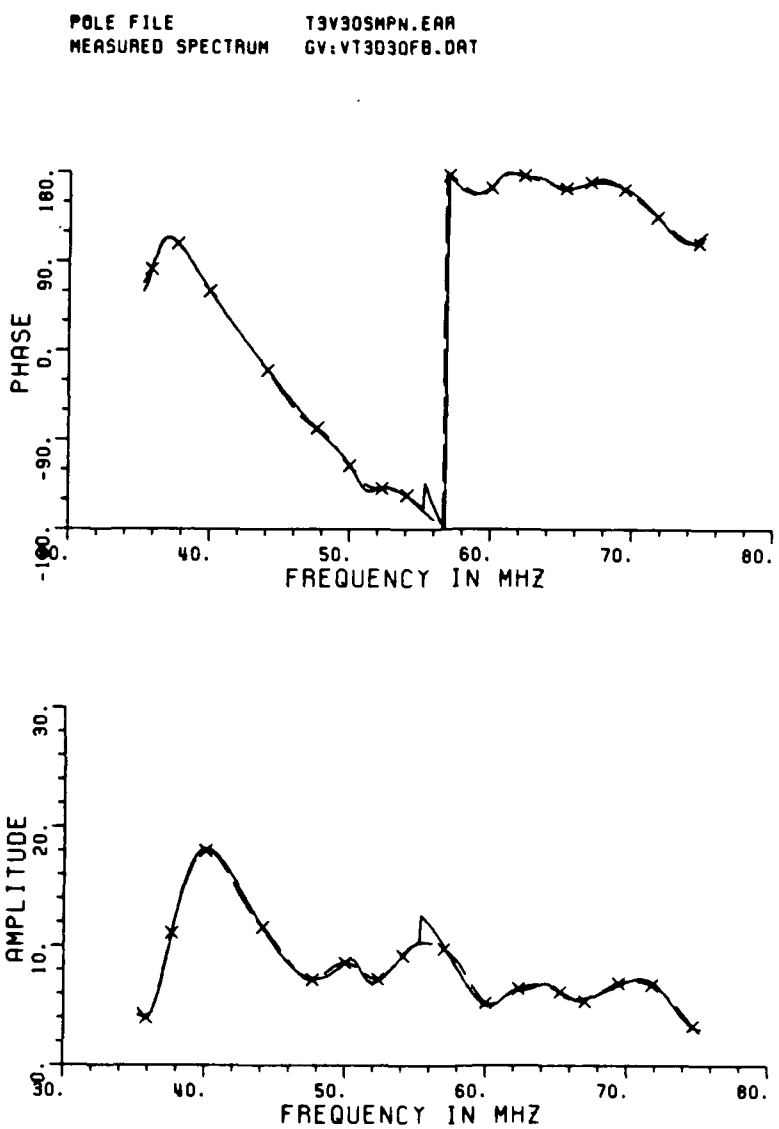

Figure 2.10. Amplitude and phase plots vs. frequency of original (dashed) and predicted (solid) spectra, for ground vehicle "T3) at an aspect angle of 30, using linear polarizaiton.

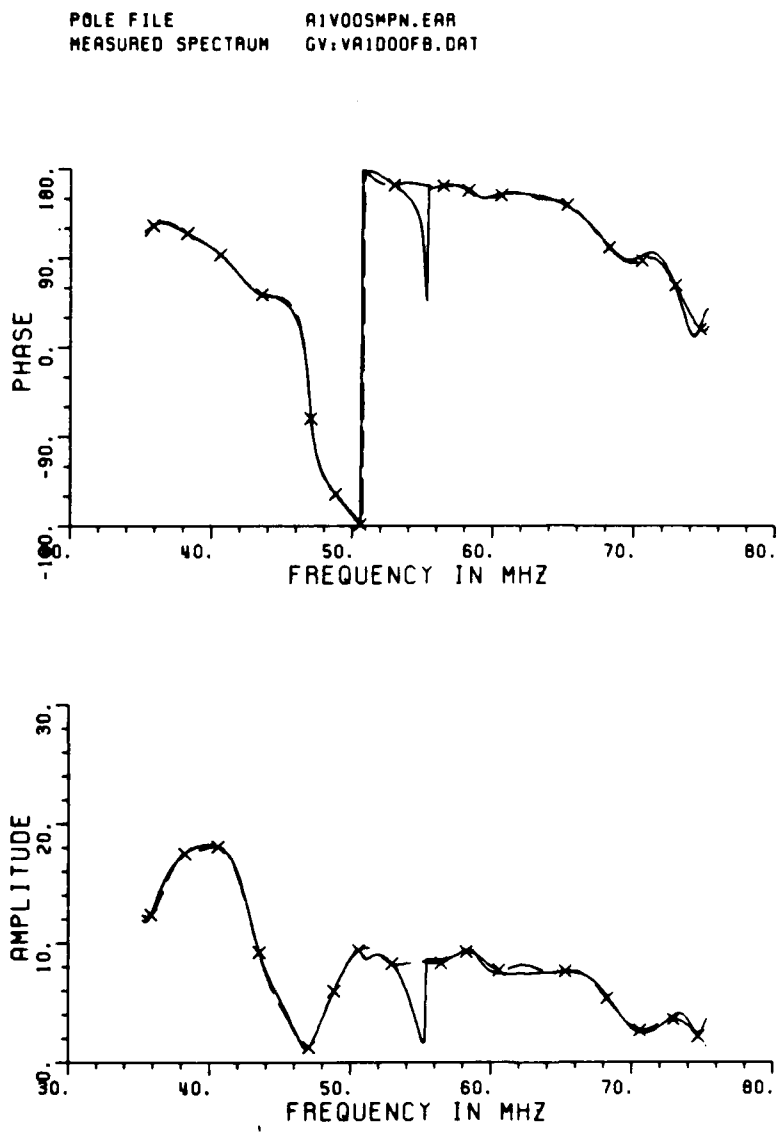

Figure 2.11. Amplitude and phase plots vs. frequency of original (dashed) and predicted (solid) spectra, for ground vehicle "A1" at an aspect angle of 0 degrees, using linear polarizaiton.

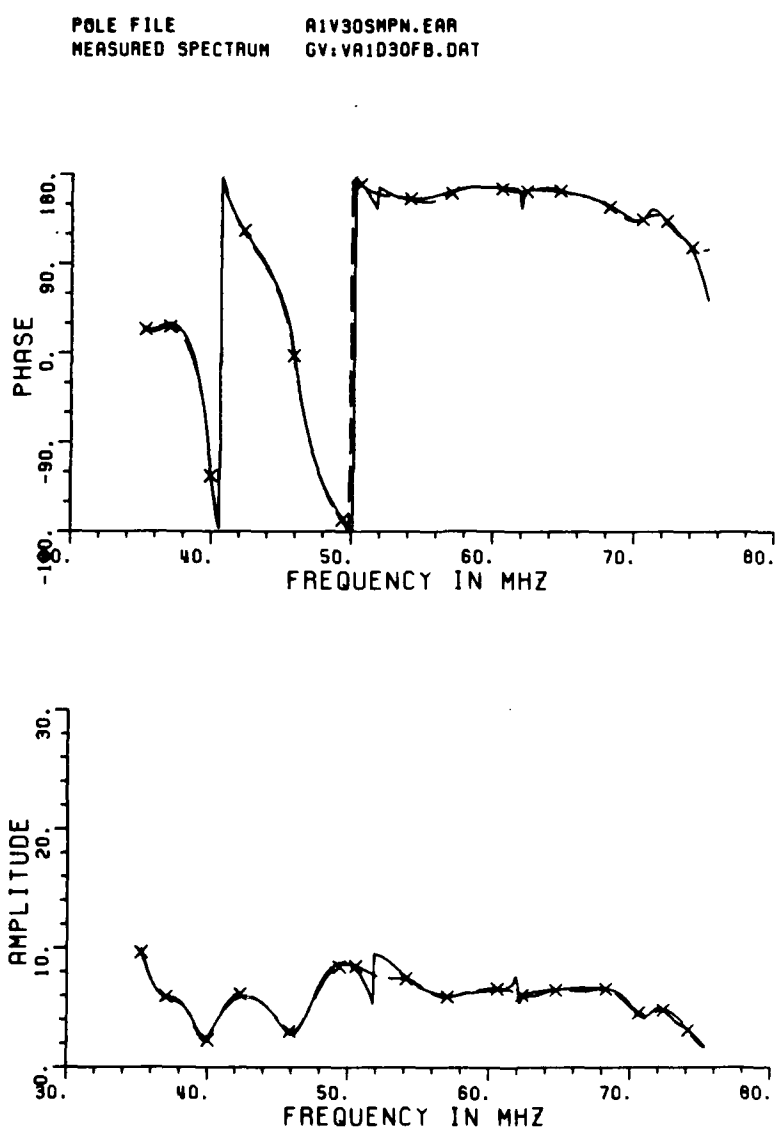

Figure 2.12. Amplitude and Phase plots vs. frequency of original (dashed) and predicted (solid) spectra, for ground vehicle "A1" at an aspect angle of 30 degrees, using linear polarization.

The approximations shown in Figures 2.7 to 2.10 are generally good however close agreement can not always be obtained for several reasons. First, the pole set may not contain all the true poles. In addition, curve fitting poles may appear in the pole set despite efforts to eliminate them. Finally the true entire function part of the response is not known and the a + bs term is not always highly succesful in approximating it. The addition of curve fitting poles usually improves the fit of a pole set to its true spectrum however experimentation has shown that this also often improves the fit to an incorrect spectrum. Thus no consistent improvement in discrimination can be achieved by adding curve fitting poles to the nominally true pole set.

In theory the poles of a scatterer are independent of the aspect angle of excitation, depending only on the physical properties of the scatterer. Real world results however are not quite so simple. Certain poles will be excited at some aspect angles and not excited or weakly excited at others. Thus the real part of a targets poles tend to vary widely from one angle to another. The oscillatory parts of a targets poles tend to remain fairly stable as can be seen in Tables 2.7 to 2.9.

TABLE 2.7

THE OSCILLATORY PARTS OF THE EXTRACTED POLES OF GROUND VEHICLE T1, WITH AVERAGE AND STANDARD DEVIATION OVER THE ASPECT ANGLE RANGE.

0	10	20	30	60	90	AVG.	STD. DEV.
2.77	2.86	2.78	2.75	2.63	2.76	2.758	(0.074)
			3.14	3.08		3.11	(0.042)
3.39		3.34	3.44	3.23		3.35	(0.0898)
3.55				3.56	3.57	3.56	(0.010)
3.76	3.63	3.66	3.76			3.70	(0.0675)
3.82	4.05	4.13		3.88	3.90	3.956	(0.129)
4.44	4.43	4.49	4.34	4.57	4.34	4.435	(0.887)
4.77	4.81					4.79	(0.0283)
	5.03	5.10	4.99	5.16	4.91	5.038	(0.0968)
5.53	5.43		5.39	5.42		5.443	(0.0608)
	5.74	5.67	5.51		5.74	5.665	(0.108)
5.90			6.19	6.14		6.077	(0.155)
	6.34	6.38			6.28	6.333	(0.0503)
6.70	6.65	6.64	6.73	6.66	6.79	6.695	(0.0575)

TABLE 2.8

THE OSCILLATORY PARTS OF THE EXTRACTED POLES OF GROUND VEHICLE T3, WITH AVERAGE AND STANDARD DEVIATION OVER THE ASPECT ANGLE RANGE.

0	10	20	30	60	90	AVG.	STD. DEV.
2.25	2.28		2.24			2.256	(0.0208)
		2.48		2.53	2.39	2.467	(0.071)
2.82	2.76			2.75	2.78	2.777	(0.031)
2.97	3.00	3.05	2.98			3.000	(0.0365)
3.24	3.31	3.19	3.28	3.17	3.25	3.24	(0.0529)
3.82	3.73	3.78	3.84		3.79	3.792	(0.0421)
		4.10		3.98	4.08	4.053	(0.0643)
4.39	4.35	4.37	4.32	4.45		4.352	(0.0928)
4.68	4.72		4.70	4.77	4.67	4.708	(0.0396)
5.05	4.99	4.93		4.98		4.988	(0.0492)
	5.42		5.22		5.31	5.32	(0.100)
	5.53		5.48	5.51		5.507	(0.0252)
5.64	5.81	5.66				5.703	(0.0929)
6.01	6.27	6.28	6.15	6.03	6.07	6.135	(0.119)
6.88	6.94	7.00	6.78	6.64	6.75	6.832	(0.133)

TABLE 2.9

THE OSCILLATORY PARTS OF THE EXTRACTED POLES OF GROUND VEHICLE A1, WITH AVERAGE AND STANDARD DEVIATION OVER THE ASPECT ANGLE RANGE.

0	10	20	30	60	90	AVG.	STD. DEV.
2.61	2.89	2.79		2.86	2.84	2.788	(0.125)
3.00		3.06	2.94	3.07		3.02	(0.060)
	3.42	3.34	3.36	3.33	3.34	3.358	(0.0363)
3.62				3.64	3.64	3.633	(0.115)
4.04	3.93	3.92	4.00		4.04	3.986	(0.0581)
4.32	4.49	4.26	4.47	4.35	4.50	4.398	(0.101)
		4.76		4.71	4.84	4.77	(0.0656)
5.00	5.06		4.92		5.08	5.015	(0.0719)
			5.27	5.21		5.24	(0.0424)
5.79	5.85	5.89		5.93	5.81	5.854	(0.0573)
5.99			6.04			6.015	(0.0353)
6.28	6.38	6.26	6.29	6.24	6.37	6.303	(0.0582)
6.57	6.69	6.75	6.72	6.59	6.79	6.685	(0.880)

CHAPTER III

DISCRIMINATION OF RADAR TARGETS

The objective of extracting poles from the measured backscatter data of various targets is to use these poles to determine an unknown target from its scattering characteristics. Discrimination algorithms have been developed in both the time and frequency domains. Mains and Moffatt [16] have applied a time domain prediction-correlation discrimination algorithm to a variety of wire-like structures. The technique used in this work is a frequency domain predictor-correlator based on a concept first suggested by J.N. Brittingham, E.K. Miller and J.L. Willows [14].

The first section of this chapter describes the frequency domian discrimination technique used and the various parameters necessary to create a predicted spectrum from a pole set. The second and third sections explain and give experimental results for discrimination in the absence of noise and in the presence of noise. The final section examines the the ability to discriminate when a targets aspect angle is uncertain.

A. FREQUENCY DOMAIN DISCRIMINATION ALGORITHM

The spectrum of a target is represented over a small bandwidth by a rational function plus an entire function

$$F(s) = \sum_{n=1}^{N} \frac{R_n}{s-p_n} + a + bs \qquad (3.1)$$

where

N is the number of LHP poles,

P_n are the extracted LHP poles,

R_n is the residue of pole P_n,

a,b are unknown real constants.

Given the set of poles P_n, the residues R_n, and the constants a and b can be obtained from $N/2 + 2$ samples of $F(jf_k)$ which is defined as

$$F(jf_k) = \sum_{n=1}^{N} \frac{R_n}{jf_k-p_n} + a + bjf_k \qquad (3.2)$$

The separation of the system of equations into imaginary and real parts allows the calculation of the residues and constants using N + 2 samples of the spectral data. Spectral data is sampled at frequencies

$$s = jf_k \qquad k = 1, \qquad N/2 + 2 \qquad (3.3)$$

which have been determined beforehand to provide a solution with the best possible fit. An 'optimum' set of sample frequencies is associated with each pole set (and consequently with each spectral data set).

Sample frequencies are generally initially chosen at or near peaks, nulls, and inflection points in the amplitude spectrum. These sample frequencies are then varied experimentally to determine an 'optimum' set. A Chebyshev solution is employed to minimize the peak error at the sampled points.

Suppose now that we are given the spectral data of an unknown target and our goal is to identify that target from a set of a priori information stored in our library. The basic idea is to construct an approximation to our unknown spectrum using the information stored in the library. The set of information which produces the closest fit to the unknown target is assumed to be the correct set thus identifying the unknown.

The parameters used in reconstructing the i^{th} target spectrum from data samples are listed below:

1) A set of dominant complex natural resonances. These are required to calculate the residues and form the rational function, and are denoted as $p_1(i)$, $p_2(i)$, ... , $p_{M_i}(i)$, where the superscript denotes the i^{th} target.

2) The model scale factor which is used in scaling the poles to full scale frequencies and denoted by SF_i.

3) Beginning, middle, and ending frequencies denoted f_b, f_m, and f_e. These denote ranges over which two separate approximations are used to cover the entire range of interest.

4) A set of optimum sample frequencies denoted as $f_1(i), f_2(i), \ldots, f_K(i)$ where $K = N_i/2 + 2$.

The frequency range of interest is divided into two sections for reconstruction due to the difficulty of approximating a range of of more than about 1.5 GHz (model frequency) with a single rational function plus a + bs. The full scale poles are obtained by dividing the model scale poles by SF_i where

$$SF_i = \frac{\text{TRUE PHYSICAL LINEAR DIMENSION OF THE } i^{th} \text{ TARGET}}{\text{MODEL LINEAR DIMENSION OF THE } i^{th} \text{ TARGET}}$$

Suppose that we are given a broadband spectral measurement of an unknown target which we wish to identify. The discrimination procedure consists of reconstructing the unknown using consecutively the data from each set stored in our library. First the unknown is sampled at the points $jf_k^{(i)}$ indicated in data set i. Then a solution is obtained for the residues R_n and the constants a and b from the relation

$$F^{(i)}(jf_k^{(i)}) = \sum_{n=1}^{N} \frac{R_n}{jf_k^{(i)} - p_n^{(i)}} + a + b\, jf_k^{(i)} \quad , \qquad (3.4)$$

where the superscript i refers to the i^{th} parameter set associated with the i^{th} target. Next a predicted spectrum is calculated over the same range as the unknown using the residues and constants a and b obtained in the previous step. The predicted spectrum is then compared with the unknown by computing a total squared error $\zeta_{i,u}$ between the unknown spectrum $F^u(jf)$ and the predicted spectrum $F^{(i)}(jf)$. This is computed as

$$\zeta_{i,u} = \frac{1}{M} \left[\sum_{m=1}^{M} \left| F^{(i)}(jf_m) - F^u(jf_m) \right|^2 \right] \quad , \qquad (3.5)$$

where M is the total number of frequency samples at which the spectra are to be compared, corresponding to

$$M = (f_e - f_b) / \Delta f \quad , \tag{3.6}$$

where Δf is the frequency increment at which measurements were originally taken. In actual processing the entire indicated range is not used for computing the error term. Rather the first and last ten percent of the range being approximated are left out of the error calculation. This is done because of the tendency of the rational function approximation to fail near the endpoints of the range being approximated, producing large errors there. Leaving a small area around the endpoints out of the error calculation leads to a number which more accurately reflects overall fit of the approximation in the more important central region of the range being considered.

Finally, a value $\tau_{i,u}$, defined as the correlation factor is computed from $\zeta_{i,u}$, as

$$\tau_{i,u} = \frac{1}{1 + \zeta_{i,u}} \tag{3.7}$$

The properties of the correlation factor $\tau_{i,u}$, are as follows. Its maximum value is unity for a predicted spectrum exactly equal to the unknown spectrum. In actuality it will never reach this value because $F^{(i)}(jf)$ is only an approximation to the unknown and the unknown will generally be corrupted by noise, further increasing the error and reducing the value of $\tau_{i,u}$. The property of $\tau_{i,u}$ used to determine the unknown is the following

$$\begin{matrix} \tau_{u,u} > \tau_{i,u} \\ \\ \zeta_{u,u} < \zeta_{i,u} \end{matrix} \qquad \forall\, i = 1,2, \ldots I \qquad i \neq u \tag{3.8}$$

The inequality (3.8) states that the total squared error will be less for a reconstruction of an unknown using poles and parameters derived from that particular spectrum than using poles and parameters derived from any other spectrum. Thus the correlation factor $\tau_{i,j}$ will be highest for the matched case where i=j, thereby identifying the unknown target.

Other criteria have been employed in calculating a correlation factor [20]. Results computed using a mean squared error criteria

$$\zeta_{i,u} = \frac{1}{M} \left| \frac{\sum_{m=1}^{M} \left| F^{(i)}(jf_m) - F^{u}(jf_m) \right|^2}{\sum_{m=1}^{M} \left| F^{u}(jf_m) \right|^2} \right| \tag{3.9}$$

do not differ significantly from those using a total squared error criteria. The numbers obtained for τ are closer to unity but the relative percentage differences are the same. An important consideration when using a total squared criteria is that the bandwidths of the various parameter sets be approximately the same so that the number of error terms appearing in τ and ζ are approximately the same.

B. DISCRIMINATION IN THE ABSENCE OF NOISE

Discrimination between radar targets in the noise free case consists of simply picking the set of poles and parameters that produces the highest correlation factor. The targets used here are three military ground vehicles denoted "T1", "T3", and "A1". The discrimination algorithm was run on target data at measured angles of 0, 10, 20, 30, 60, and 90 degrees. The correlation factors $\tau_{i,j}$ resulting from these data runs are given in Tables 3.1 and 3.2 where the subscripts i and j correspond to the i^{th} spectrum and the j^{th} pole set. As expected each diagonal element, corresponding to the pole set matched to the spectrum, produces a higher correlation factor than for either incorrect pole set in the column. It may be expected that the larger the difference between the matched and unmatched correlation factors the better will be the discrimination as noise is added to the test spectrum.

C. DISCRIMINATION IN THE PRESENCE OF NOISE

In order to model an actual radar discrimination situation as closely as possible the effect of noise or error must be considered in our simulation. To approximate noise, a computer program was used to generate Gaussian distributed random numbers of zero mean and standard deviation σ. The probability density function of such a distribution will have the form

TABLE 3.1

CORRELATION FACTOR FOR GROUND VEHICLES
T1, T3, AND A1 FOR NON-NOISY DATA

Spectral Data / Pole Set	T1	T3	A1
T1	0.8140	0.7517	0.7698
T3	0.7982	0.9265	0.7604
A1	0.4159	0.6818	0.8646

(a) 0° Aspect Angle

Spectral Data / Pole Set	T1	T3	A1
T1	0.7336	0.8500	0.4618
T3	0.6061	0.9009	0.4357
A1	0.1793	0.4396	0.7909

(b) 10° Aspect Angle

Spectral Data / Pole Set	T1	T3	A1
T1	0.7960	0.5882	0.5297
T3	0.4654	0.8281	0.6498
A1	0.3099	0.7659	0.9124

(c) 20° Aspect Angle

TABLE 3.2

CORRELATION FACTOR FOR GROUND VEHICLES
T1, T3, AND A1 FOR NON-NOISY DATA

Spectral Data / Pole Set	T1	T3	A1
T1	0.5944	0.6565	0.4308
T3	0.3939	0.8739	0.6383
A1	0.2386	0.6050	0.8857

(a) 30° Aspect Angle

Spectral Data / Pole Set	T1	T3	A1
T1	0.7821	0.5128	0.6669
T3	0.1407	0.7581	0.1389
A1	0.2181	0.6615	0.8390

(b) 60° Aspect Angle

Spectral Data / Pole Set	T1	T3	A1
T1	0.4376	0.3139	0.0811
T3	0.1071	0.4655	0.0709
A1	0.4108	0.3574	0.4826

(c) 90° Aspect Angle

$$F(z) = \frac{1}{2\pi\sigma^2} e^{-z^2/2\sigma^2} \tag{3.10}$$

The computer generated random numbers are added to the real and imaginary parts of the spectral data, using a different seed for each. The complex phasor form of a noiseless spectrum H(f) can be written as real and imaginary parts

$$\tilde{H}(f) = R(f) + jC(f) \tag{3.11}$$

If the noise is also written in terms of its imaginary and real parts

$$\tilde{N} = N_R + j\tilde{N}_C \tag{3.12}$$

where N_R and N_C are the two independently generated sets of real random numbers. The resulting noisy data becomes

$$\tilde{H}(f) = [R(f) + N_R] + j[C(f) + N_C] \tag{3.13}$$

To obtain a relation between the signal to noise ratio (SNR), and the standard deviation σ of the Gaussian distributed random numbers it is necessary to compute signal power and noise power. The signal power is defined as

$$P_s = \langle |H(X_i)|^2 \rangle \tag{3.14}$$

where <a> is defined as the average of quantity a, and $X_i = jf_i$. For this application the spectral data is discrete therefore

$$P_s = \frac{1}{M_d} \left[\sum_{i=1}^{M_d} [A(X_i)]^2 \right] \tag{3.15}$$

where M_d is the total number of data samples in the spectrum, and $A(X_i)$ is the amplitude of the phasor $H(X_i)$. The noise power is defined in a similar manner

$$P_N = \langle|\tilde{N}|^2\rangle \quad , \tag{3.16}$$

$$P_N = \langle|N_R + jN_C|^2\rangle \quad , \tag{3.17}$$

$$P_N = \langle N_R^2\rangle + \langle N_C^2\rangle \quad , \tag{3.18}$$

Since N_R and N_C are independent Gaussian distributed random variables with a standard deviation of σ, it follows that

$$\langle N_R^2\rangle = \sigma^2 = \langle N_C^2\rangle \tag{3.19}$$

Therefore the noise power is

$$P_N = 2\,\sigma^2 \tag{3.20}$$

Thus the signal to noise ratio (SNR) in decibels is

$$SNR = 10 \log_{10} \left[\frac{P_s}{P_N} \right] \tag{3.21}$$

$$SNR = 10 \log_{10} \left[\frac{1}{2\sigma^2 M_d} \left[\sum_{i=1}^{M_d} [A(X_i)]^2 \right] \right] \tag{3.22}$$

Solving for the standard deviation in terms of (SNR), we get

$$\sigma = \sqrt{\frac{\frac{1}{M_d} \sum_{i=1}^{M_d} [A(X_i)]^2}{2 \times 10^{(SNR/10)}}} \tag{3.23}$$

The discrimination algorithm is tested against noisy data using a program which adds noise to a spectral file and then constructs a predicted spectrum using sets of poles and parameters from the library. Say that we want to identify a spectrum, designated A, from a library of pole sets designated B, C, and D. The program accepts the spectral file A and adds Gaussian noise to it as previously described. Then a predicted spectrum is constructed and a correlation factor calculated using in turn each of the pole files B, C, and D. If the correlation factor is highest for the pole set corresponding to the spectrum A then a correct identification is tallied. This process is repeated, using different noise seeds, ten times at each noise to signal ratio. The probability of classification at each noise to signal ratio is then the number of correct identifications out of ten.

Plots of classification percentage versus aspect angle for various noise to signal ratios are shown in Figures 3.1 to 3.3. Note the expected relationship between the classification results and the correlation factor separation in the noiseless case. For example Figure 3.1 shows that the classification of target T1 at 60 degrees is much better than at 90 degrees. Looking at Table 3.2 we see that the matched case correlation factor is 0.7821 and the largest unmatched case correlation factor is for the pole set of A1 vs the spectrum of T1, a value of 0.2181. Thus the separation is 0.5640. At 90 degrees the T1 matched case correlation factor is 0.4376 while the largest unmatched case correlation factor is again for pole set A1 vs the spectrum of T1, a value of 0.4108, resulting in a separation of only 0.0272. Similar results are found for other cases where a high failure rate is observed.

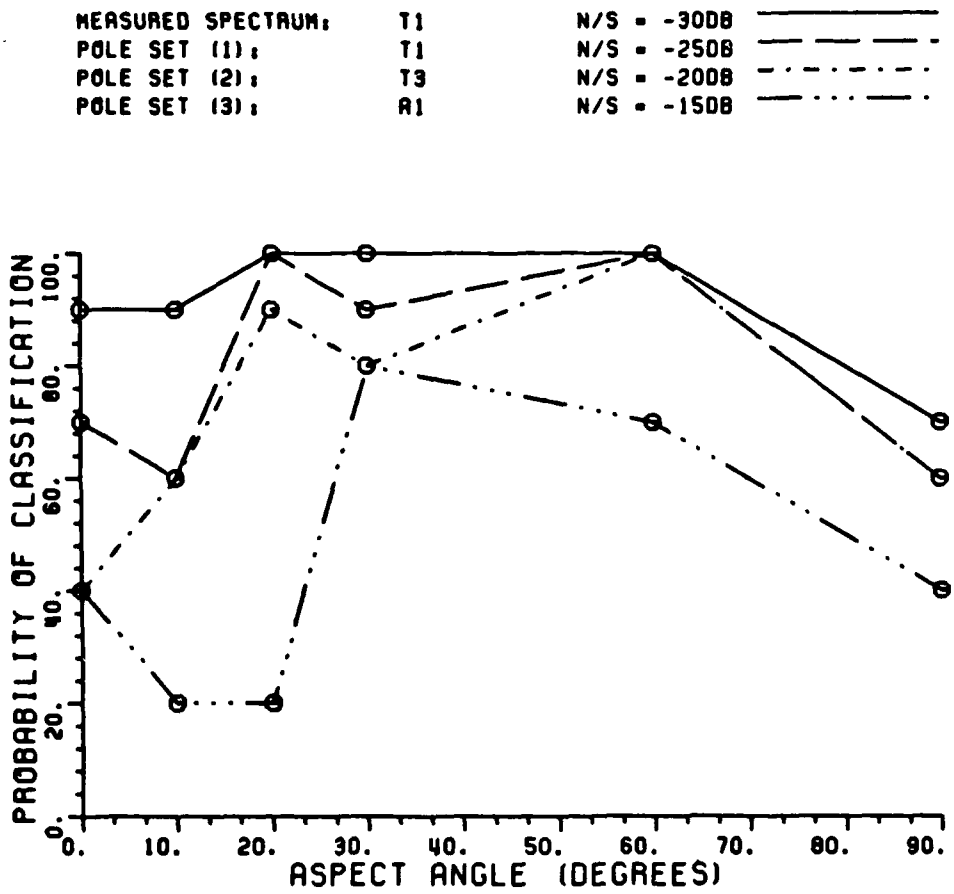

Figure 3.1. Probability of classification versus aspect angle for target T1. This set of curves indicates the probability of classifying target T1, for the indicated noise to signal ratios, from the pole sets of targets T1, T3, and A1.

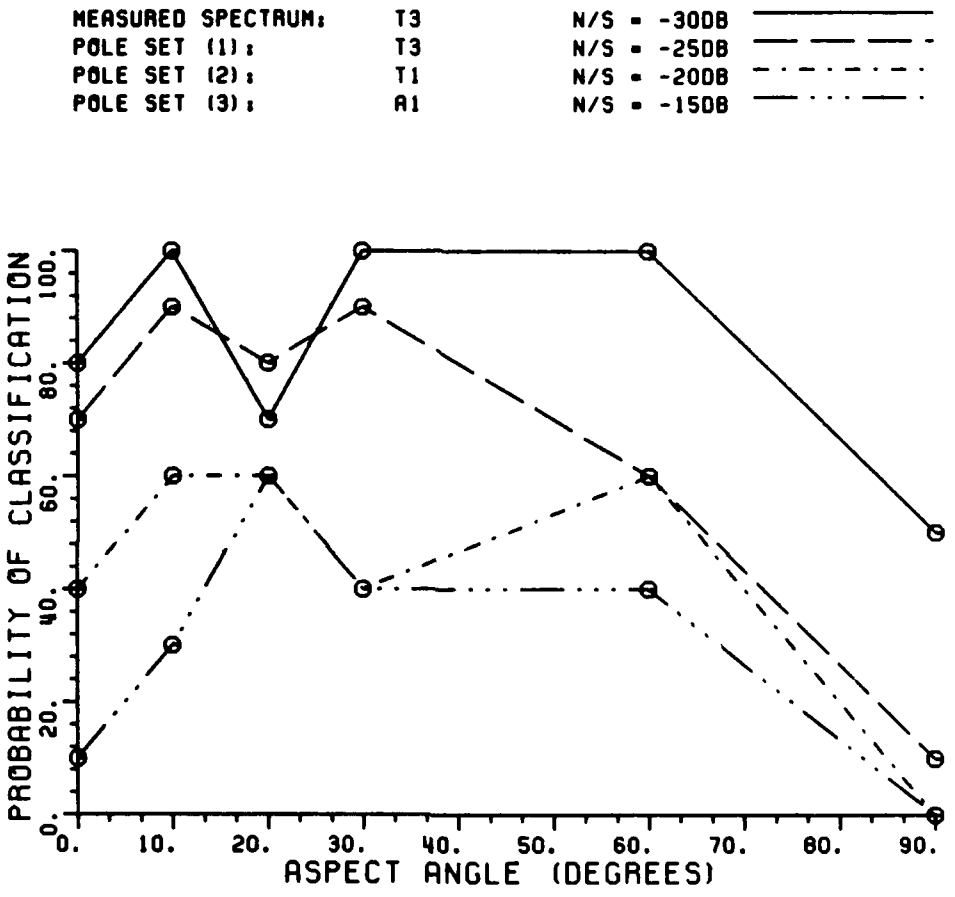

Figure 3.2. Probability of classification versus aspect angle for target T3. This set of curves indicates the probability of classifying target T3, for the indicated noise to signal ratios, from the pole sets of targets T1, T3, and A1.

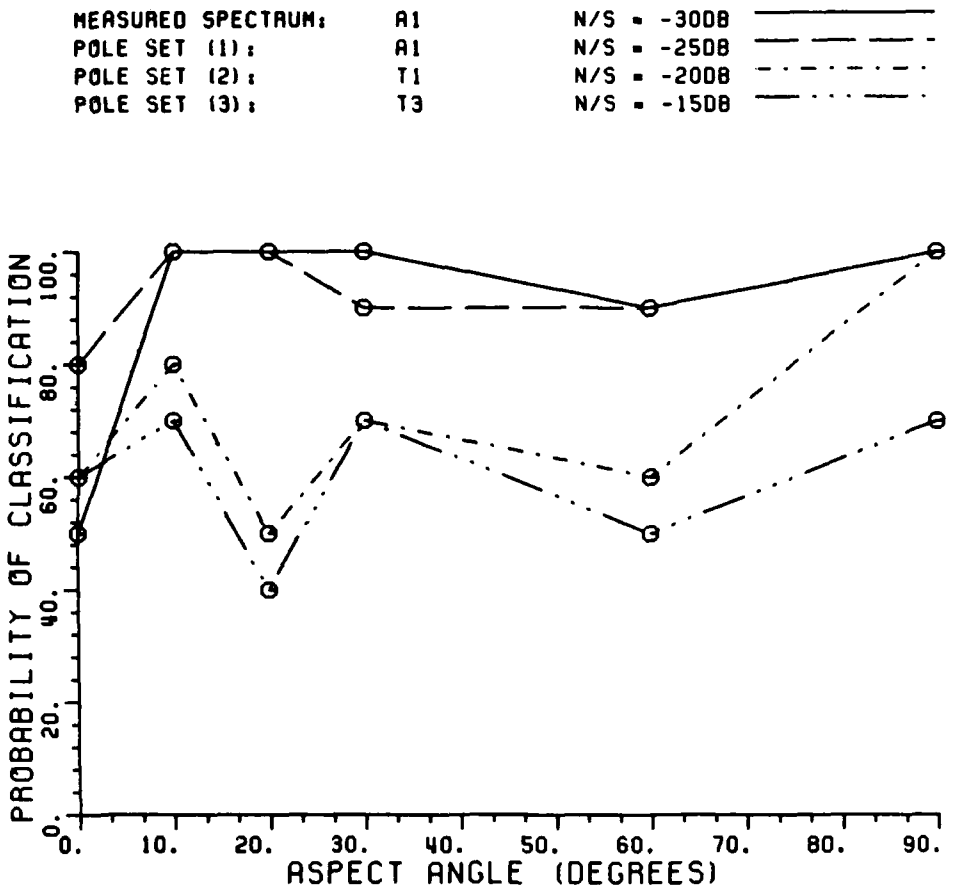

Figure 3.3. Probability of classification versus aspect angle for target A1. This set of curves indicates the probability of classifying target A1, for the indicated noise to signal ratios, from the pole sets of targets T1, T3, and A1.

D. EFFECTS OF POLE VARIATION IN DISCRIMINATION

The ability to discriminate between targets with a known aspect angle has been shown. However it may not always be possible to determine a targets aspect angle exactly, some degree of error is to be expected. Given this, it is pertinent to examine the degree to which discrimination may be achieved using pole sets of angles adjacent to the aspect angle of the measured spectrum. The noise-free correlation factors for adjacent angle cases between 0 and 30 degrees are presented in Tables 3.3 to 3.8.

The results here are quite variable, however certain trends can be seen. Note in Table 3.3 that the T1 10 degree pole set fits the A1 0 degree spectrum much better than the A1 10 degree pole set. Likewise in Table 3.4 the T1 0 degree pole set fits the A1 10 degree spectrum better than the A1 0 degree pole set.

This result may be due in part to the fact that in each of these cases the T1 pole sets use more poles in their approximations than the same angle A1 pole sets. The question of which poles are critical to the approximation of a given response, which poles may be expendable, and which are most important in discrimination is still very much open.

TABLE 3.3

CORRELATION FACTOR FOR SPECTRA VERSUS ADJACENT ANGLE POLE SETS.
FACTORS FOR 0 DEGREE SPECTRA VERSUS 10 DEGREE POLE SETS.

Spectrum	Pole set	Correlation factor
T1 0 deg	T1 10 deg	0.7064
T1 0 deg	T3 10 deg	0.7525
T1 0 deg	A1 10 deg	0.2207
T3 0 deg	T3 10 deg	0.9049
T3 0 deg	T1 10 deg	0.6939
T3 0 deg	A1 10 deg	0.3932
A1 0 deg	A1 10 deg	0.3996
A1 0 deg	T1 10 deg	0.7404
A1 0 deg	T3 10 deg	0.5457

TABLE 3.4

CORRELATION FACTOR FOR SPECTRA VERSUS ADJACENT ANGLE POLE SETS.
FACTORS FOR 10 DEGREE SPECTRA VERSUS 0 DEGREE POLE SETS.

Spectrum	Pole set	Correlation factor
T1 10 deg	T1 0 deg	0.8346
T1 10 deg	T3 0 deg	0.6833
T1 10 deg	A1 0 deg	0.4573
T3 10 deg	T3 0 deg	0.9347
T3 10 deg	T1 0 deg	0.7382
T3 10 deg	A1 0 deg	0.5997
A1 10 deg	A1 0 deg	0.4586
A1 10 deg	T1 0 deg	0.7918
A1 10 deg	T3 0 deg	0.7739

TABLE 3.5

CORRELATION FACTOR FOR SPECTRA VERSUS ADJACENT ANGLE POLE SETS.
FACTORS FOR 10 DEGREE SPECTRA VERSUS 20 DEGREE POLE SETS.

Spectrum	Pole set	Correlation factor
T1 10 deg	T1 20 deg	0.7570
T1 10 deg	T3 20 deg	0.4783
T1 10 deg	A1 20 deg	0.3094
T3 10 deg	T3 20 deg	0.5026
T3 10 deg	T1 20 deg	0.7326
T3 10 deg	A1 20 deg	0.8044
A1 10 deg	A1 20 deg	0.8079
A1 10 deg	T1 20 deg	0.5629
A1 10 deg	T3 20 deg	0.7289

TABLE 3.6

CORRELATION FACTOR FOR SPECTRA VERSUS ADJACENT ANGLE POLE SETS.
FACTORS FOR 20 DEGREE SPECTRA VERSUS 10 DEGREE POLE SETS.

Spectrum	Pole set	Correlation factor
T1 20 deg	T1 10 deg	0.6505
T1 20 deg	T3 10 deg	0.6287
T1 20 deg	A1 10 deg	0.1673
T3 20 deg	T3 10 deg	0.9357
T3 20 deg	T1 10 deg	0.5529
T3 20 deg	A1 10 deg	0.3303
A1 20 deg	A1 10 deg	0.6667
A1 20 deg	T1 10 deg	0.6557
A1 20 deg	T3 10 deg	0.4779

TABLE 3.7

CORRELATION FACTOR FOR SPECTRA VERSUS ADJACENT ANGLE POLE SETS.
FACTORS FOR 20 DEGREE SPECTRA VERSUS 30 DEGREE POLE SETS.

Spectrum	Pole set	Correlation factor
T1 20 deg	T1 30 deg	0.3096
T1 20 deg	T3 30 deg	0.3522
T1 20 deg	A1 30 deg	0.1659
T3 20 deg	T3 30 deg	0.7789
T3 20 deg	T1 30 deg	0.6331
T3 20 deg	A1 30 deg	0.4204
A1 20 deg	A1 30 deg	0.6902
A1 20 deg	T1 30 deg	0.3609
A1 20 deg	T3 30 deg	0.5966

TABLE 3.8

CORRELATION FACTOR FOR SPECTRA VERSUS ADJACENT ANGLE POLE SETS.
FACTORS FOR 30 DEGREE SPECTRA VERSUS 20 DEGREE POLE SETS.

Spectrum	Pole set	Correlation factor
T1 30 deg	T1 20 deg	0.6288
T1 30 deg	T3 20 deg	0.4403
T1 30 deg	A1 20 deg	0.3934
T3 30 deg	T3 20 deg	0.7838
T3 30 deg	T1 20 deg	0.7691
T3 30 deg	A1 20 deg	0.8275
A1 30 deg	A1 20 deg	0.8752
A1 30 deg	T1 20 deg	0.5973
A1 30 deg	T3 20 deg	0.7438

CHAPTER IV

SUMMARY, CONCLUSIONS AND RECOMMENDATIONS

The purpose of this study was the testing of a method of target discrimination using Complex Natural Resonances (CNR's). The discrimination technique employed here is a prediction-correlation algorithm utilizing poles extracted from measured target scattering data. The targets used were three military ground vehicles.

Broadband target scattering data are obtained on a compact range and calibrated by background subtraction and normalization with respect to a sphere. Ground plane edge diffraction effects and other clutter not removed during calibration were removed using a frequency domain digital filter which corresponds to a tenth order butterworth time domain window.

Poles were extracted from frequency domain data using a rational function approximation. Setting the numerator order one greater than the denominator is equivalent to the inclusion of an entire function of order one (i.e., a + bs). The entire function is a simple attempt to model the forced response part of a target' s overall response. Poles are extracted in overlapping frequency domain windows to help eliminate curve fitting poles. The real parts of extracted poles are observed to

vary with aspect angle. Although some poles are not excited at every aspect angle the oscillatory parts of the poles remain relatively stable.

Given an unknown response, target discrimination consists of the construction of a predicted response, using previously extracted pole sets, followed by the comparison of the predicted response with the unknown's response. The predicted response is a rational function approximation in which the residues and constants are calculated using the unknown's response and a set of poles and sample frequencies. As in the extraction of poles, an entire function a + bs is included to improve the approximation. A Chebyshev solution, which minimizes the maximum error, is employed in the calculation of the residues and constants. The set of sample frequencies corresponding to each pole set was previously optimized to provide the best possible fit, in the mean-square sense, to the spectrum which corresponds to that pole set. The bandwidth of interest is broken into two two sections, each approximated by a separate function, due to the difficulty of approximating a range of more than about 1.5 GHz with one rational function. A correlation factor is calculated for the predicted response using each of the possible pole sets. The pole set realizing the highest correlation factor identifies the target.

Testing of the discrimination algorithm against noisy data is accomplished by adding computer generated white Gaussian noise to the unknown spectra. Ten different noise seeds were tested at each noise to signal ratio in order to obtain a statistically significant sample.

Successful discrimination is demonstrated for low noise to signal ratios at all tested angles with the exception of 0 and 90 degrees, i.e., nose-on and broadside. Discrimination fails at various rates as noise to signal ratio is increased. Best case discrimination is achieved where the seperation between the (noiseless) correlation factors for the matched case and the unmatched case is the greatest.

Although certain basic principles apply in the choice of sample points (i.e., peak, null, and inflection points are generally good choices), optimizing the sample points is still a trial and error procedure indicating the need for further study in this area. In this work the frequency range utilized in discrimination was the same for each target. The fact that certain frequency ranges were more amenable to a good fit than others points out the need for study into the question of what frequency range(s) are most effective in discrimination.

The extraction of poles from experimental data is well established; There is much room for improvement however, in finding an optimal pole set. The fact that cross-polarized measurements have reduced speculars as opposed to co-polarized measurements leads to the question of whether poles might be more effectively extracted from cross-polarized data. Unfortunately cross-polarized data of the targets used here was not available at the time of this study.

Although the best way to use CNR's in discrimination has not yet been determined the results presented here show significant potential and define some areas for future research.

APPENDIX A

IDENTIFICATION OF RESONANT SUBSTRUCTURES

In this appendix certain target structures and substructures are associated with certain extracted poles. The structures and substructures are not identified explicitly for security classification reasons, but are refered to by reference designations; f1, f2, etc. Tables A.1, A.2, and A.3 give the results for targets T1, T3, and A1 respectively. All dimensions and frequencies are model scale. The first column gives the reference designation for the relevant structure. The second column gives the approximate physical length of the structure as measured on the target model. The third column gives the the dipole first resonant frequency of the length given in column two. The following three columns give the oscillatory part of a pole which is near in frequency to the frequency given in column three, and a percentage difference from the column three frequency, utilizing pole sets extracted at 0, 10, and 20 degrees aspect angle.

Although the structures refered to in this appendix are generally quite unlike a dipole in shape the calculation of a dipole resonant frequency gives a first approximation in relating poles to possible resonant structures on a given target. Confirmation of the relationship

of a given structure to one or more extracted poles would require the modification of that structure on the model target and a re-measurement of the RCS over the band of interest. After re-measurment poles would again be extracted and differences between the original and new pole set would be noted.

TABLE A.1

LENGTH, CORRESPONDING FIRST RESONANT FREQUENCY AND OSCILLATORY PART OF POSSIBLE CORRESPONDING POLE FOR SOME FEATURES OF TARGET T1. PERCENTAGE DIFFERENCE IS THE DIFFERENCE BETWEEN THE OSCILLATORY PART OF THE EXTRACTED POLE AND 'NATURAL' RESONANT FREQUENCY OF THE FEATURE LENGTH ASSUMING A DIPOLE TYPE RESONANCE.

		First Resonant	0 degrees		10 degrees		20 degrees	
Ref.	Length (meters)	Frequency (Ghz)	Pole (Ghz)	Percent Diff.	Pole (Ghz)	Percent Diff.	Pole (Ghz)	Percent Diff.
f1	0.040	3.75	-	-	3.68	1.9%	-	-
f2	0.030	5.00	5.15	3.0%	5.00	0%	5.07	1.4%
f3	0.045	3.33	-	-	-	-	3.43	3.0%
f4	0.029	5.17	5.15	0.4%	5.27	1.9%	5.07	2.0%
f5	0.0445	3.37	3.50	3.8%	-	-	3.43	1.7%

TABLE A.2

LENGTH, CORRESPONDING FIRST RESONANT FREQUENCY AND OSCILLATORY PART OF POSSIBLE CORRESPONDING POLE FOR SOME FEATURES OF TARGET T3. PERCENTAGE DIFFERENCE IS THE DIFFERENCE BETWEEN THE OSCILLATORY PART OF THE EXTRACTED POLE AND 'NATURAL' RESONANT FREQUENCY OF THE FEATURE LENGTH ASSUMING A DIPOLE TYPE RESONANCE.

		First Resonant	0 degrees		10 degrees		20 degrees	
Ref.	Length (meters)	Frequency (Ghz)	Pole (Ghz)	Percent Diff.	Pole (Ghz)	Percent Diff.	Pole (Ghz)	Percent Diff.
g1	0.070	2.14	2.24	4.6%	2.22	3.7%	-	-
g2	0.0286	5.24	5.55	5.9%	-	-	-	-
g3	0.0254	5.91	-	-	-	-	5.71	3.3%
g4	0.0222	6.76	6.81	0.7%	6.85	1.3%	-	-
g5	0.035	4.29	4.25	0.1%	4.25	0.1%	4.24	0.12%

TABLE A.3

LENGTH, CORRESPONDING FIRST RESONANT FREQUENCY AND OSCILLATORY PART OF POSSIBLE CORRESPONDING POLE FOR SOME FEATURES OF TARGET A1. PERCENTAGE DIFFERENCE IS THE DIFFERENCE BETWEEN THE OSCILLATORY PART OF THE EXTRACTED POLE AND 'NATURAL' RESONANT FREQUENCY OF THE FEATURE LENGTH ASSUMING A DIPOLE TYPE RESONANCE.

		First Resonant	0 degrees		10 degrees		20 degrees	
Ref.	Length (meters)	Frequency (Ghz)	Pole (Ghz)	Percent Diff.	Pole (Ghz)	Percent Diff.	Pole (Ghz)	Percent Difference
h1	0.054	2.78	2.72	2.1%	2.72	2.1%	2.61	4.0%
h2	0.0318	4.72	-	-	4.75	0.6%	-	-
h3	0.0254	5.91	5.71	3.4%	-	-	5.91	0%

APPENDIX B

IMPROVING DISCRIMINATION BETWEEN TWO TARGETS

Discriminating between two targets at a time is simpler than discriminating among a larger number of targets. Given only two targets and correspondingly only two pole sets it is simpler to adjust the parameters of the pole sets to give a high correlation factor with the correct target and at the same time a low correlation factor with the (one) incorrect target. This would result in a total of six sets of poles/parameters for three targets. The results of such an investigation are enlightening if not necessarily directly practical.

One approach to improving discrimination between two targets is the elimination of one or more poles in cases where certain poles from two different pole sets are very close. This is illustrated by Figures B.1 and B.2 where pole locations for targets are plotted for comparison purposes (only the positve half of the imaginary axis is shown, each pole plotted has a complex conjugate pole with a negative imaginary part). Note in Figure B.1 that pole set T1 at 0 degrees has pole pairs at -.196 +/-j3.55 and at -.199 +/-j3.82 while T3 at 0 degrees has pole pairs very close to these at -.173 +/-j3.57 and at -.183 +/-j3.82.

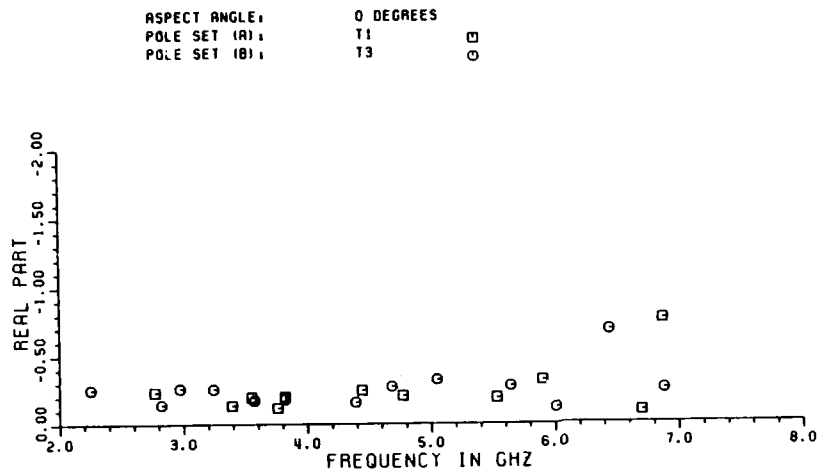

Figure B.1 Plot of pole locations for targets T1 and T3.

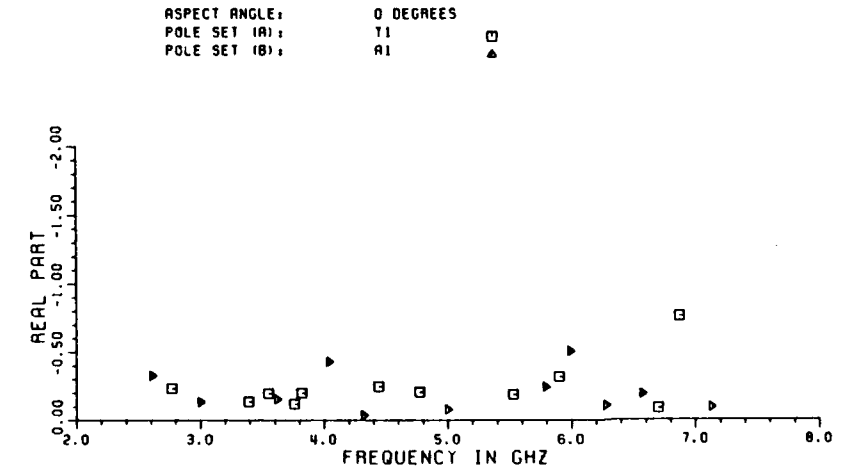

Figure B.2 Plot of pole locations for targets T1 and A1.

Figure B.2 shows that the T1 0 degree pole pair at -.196 +/-j3.55 is very close to the A1 0 degree pole pair at -.153 +/-j3.62.

Eliminating one or more pole pairs from a pole set almost always degrades the fit that can be obtained (as measured by the correlation factor) but sometimes a better separation between the correct case and incorrect case correlation factors can be obtained. The results of eliminating the above mentioned pole pairs in T1 and T3 and running the discrimination algorithm are shown in Table B.1 The correlation factor separation when T1 is the target spectrum is improved (see Table 3.1) but the separation obtained when T3 is the target spectrum is no better than before. On the other hand if we take the two possible targets T1 and A1 and eliminate only the T1 pole pair at -.196 +/-3.55, the separation between the matched and unmatched cases is improved for both spectra as shown in Table B.2 (compare Table 3.1).

Figures B.3 through B.6 confirm our expectations with respect to discrimination in the presence of noise. Discrimination between targets T1 and A1 is improved with the elimination of the T1 pole pair at -.196 +/-j3.55. In particular for the case of A1 as the target spectrum, no consistent discrimination could be said to have been achieved previously, however in the new case discrimination is consistent out to a -25 dB noise to signal ratio. Figures B.5 and B.6 show a different story for the discrimination between T1 and T3 when the T1 pole pairs at -.196 +/-j3.55 and at -.199 +/-j3.82 and the T3 pole pairs at-.173

TABLE B.1

CORRELATION FACTORS FOR POLE SETS T1 AND T3
AT 0 DEGREES WITH CERTAIN POLES ELIMINATED

Spectral Data / Pole Set	T1	T3
T1	0.5277	0.7576
T3	0.1259	0.8553

TABLE B.2

CORRELATION FACTORS FOR POLE SETS T1 AND A1
AT 0 DEGREES WITH CERTAIN POLES ELIMINATED

Spectral Data / Pole Set	T1	A1
T1	0.6879	0.4531
A1	0.4159	0.8646

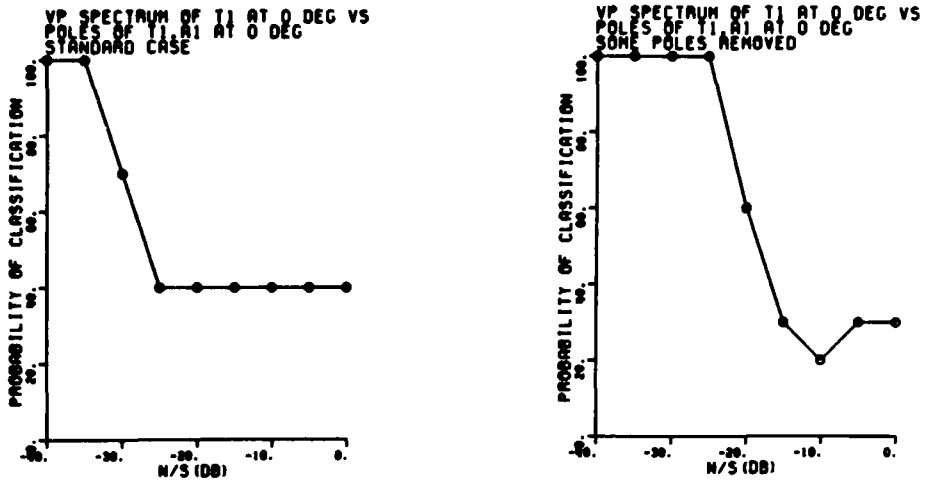

Figure B.3 Probability of classification versus noise to signal ratio for the spectrum of target T1 versus the poles of T1 and A1. Standard case (a), case with some poles removed (b).

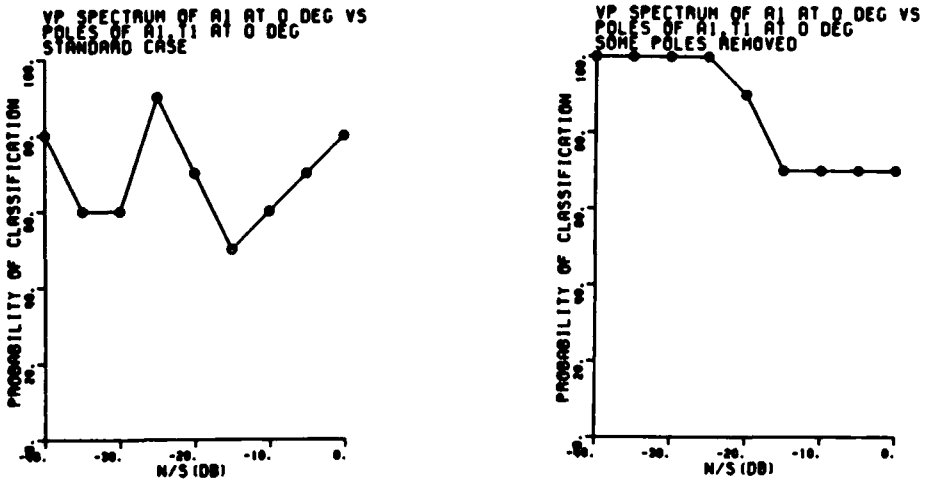

Figure B.4 Probability of classification versus noise to signal ratio for the spectrum of target A1 versus the poles of A1 and T1. Standard case (a), case with some poles removed (b).

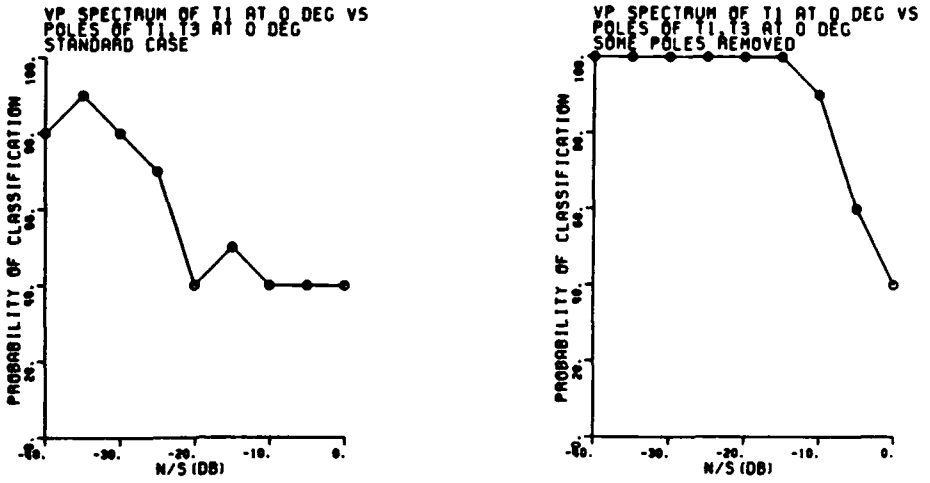

Figure B.5 Probability of classification versus noise to signal ratio for the spectrum of target T1 versus the poles of T1 and T3. Standard case (a), case with some poles removed (b).

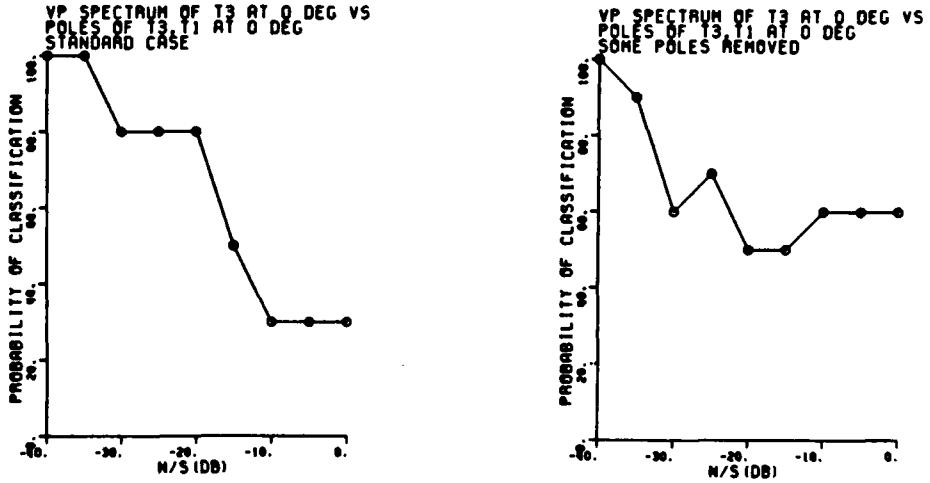

Figure B.6 Probability of classification versus noise to signal ratio for the spectrum of target T3 versus the poles of T3 and T1. Standard case (a), case with some poles removed (b).

+/-j3.57 and at -.183 +/-j3.82 are eliminated. The ability to recognize the target T1 is much improved but this is at the expense of slightly degraded the ability to recognize T3, thus there is no overall improvement in discrimination.

Plots of probability of classification versus aspect angle for targets taken two at a time are shown in Figures B.7 through B.12. The cases marked (a) are simply the results of section 3-C broken down for targets two at a time. In the cases marked (b) the improvement techniques of this section have been applied for some cases at some aspect angles. The pole elimination technique was actually tried for all the cases, where no improvment was obtained (as in the 0 degree T1 and T3 case above) the original results were taken to be best case and plotted, however when improvement was obtained the improved results were taken to be best case and plotted. Significant improvements were obtained in the discrimination between T1 and T3 at 90 degrees, between T1 and A1 at 0, 20, 60, and 90 degrees, between A1 and T3 at 20 degrees.

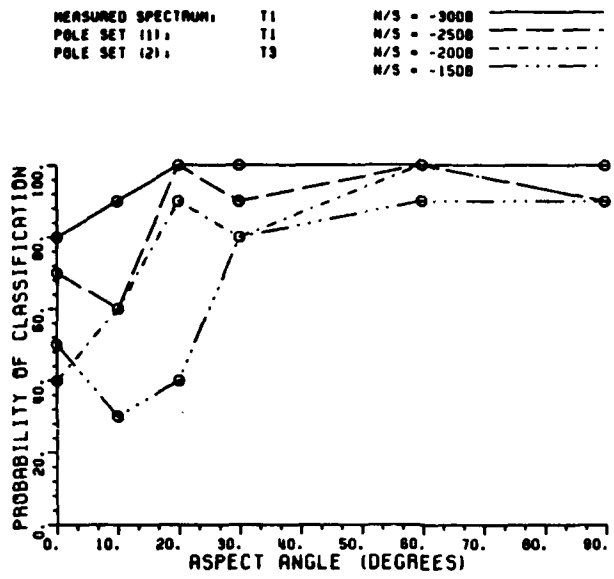

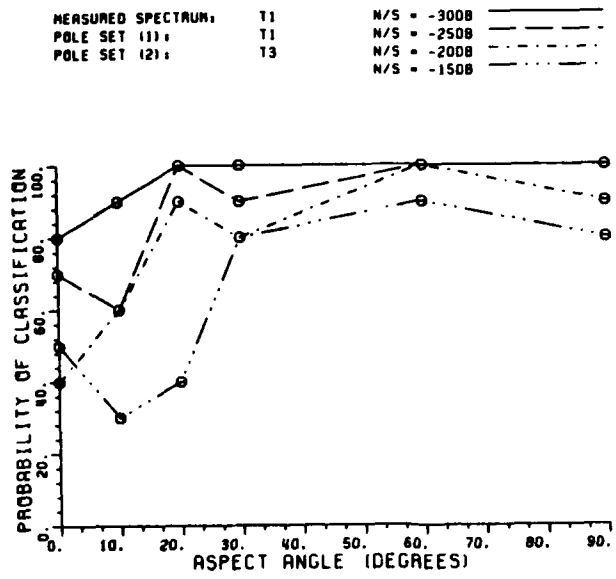

Figure B.7 Probability of classification versus aspect angle for the spectrum of target T1 versus the poles of T1 and T3. Standard case (a), case with some poles removed at certain aspect angles (b).

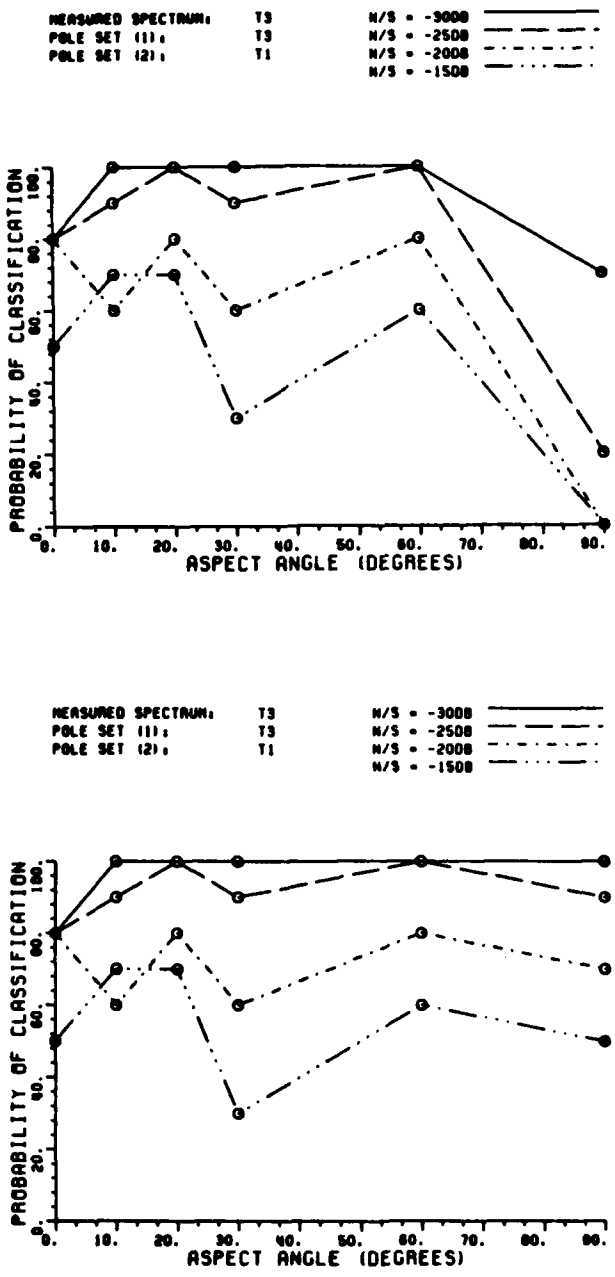

Figure B.8 Probability of classification versus aspect angle for the spectrum of target T3 versus the poles of T3 and T1. Standard case (a), case with some poles removed at certain aspect angles (b).

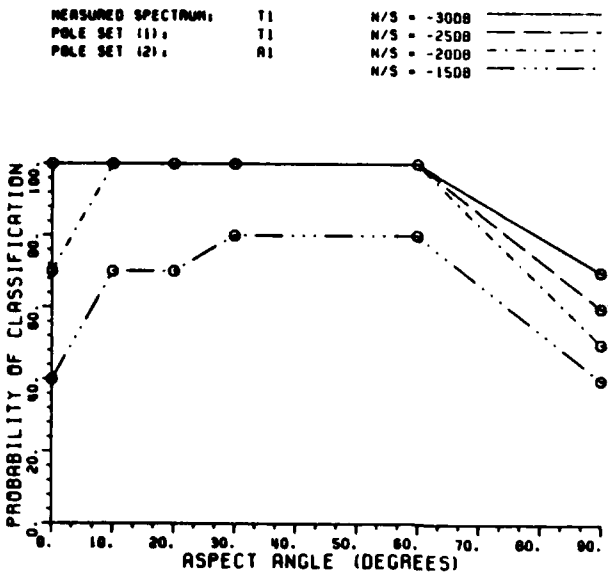

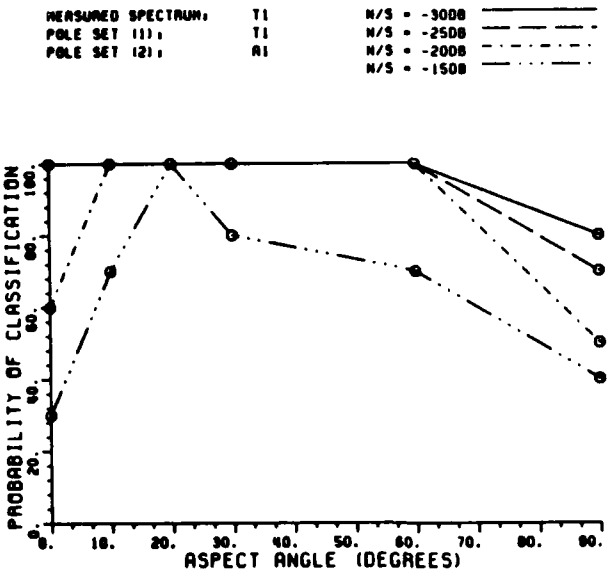

Figure B.9 Probability of classification versus aspect angle for the spectrum of target T1 versus the poles of T1 and A1. Standard case (a), case with some poles removed at certain aspect angles (b).

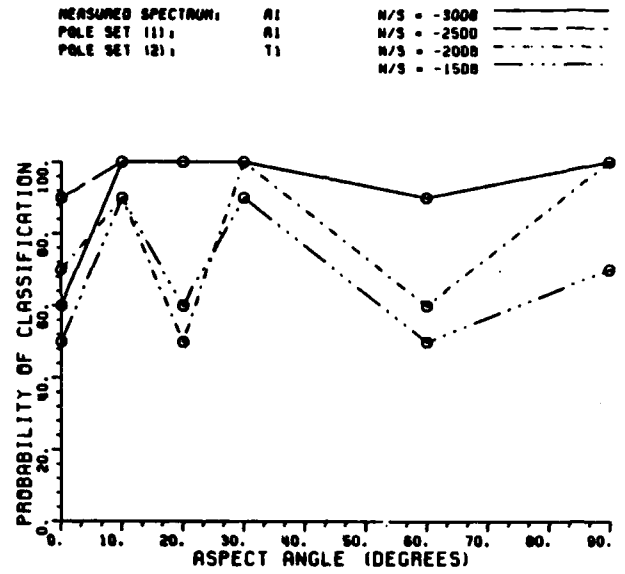

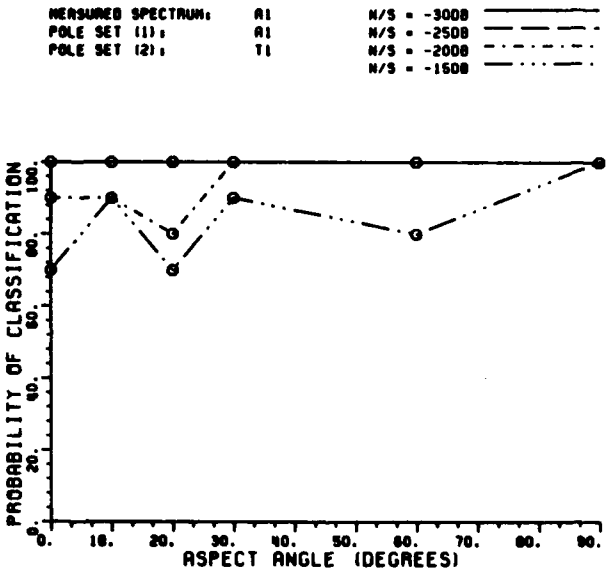

Figure B.10 Probability of classification versus aspect angle for the spectrum of target A1 versus the poles of A1 and T1. Standard case (a), case with some poles removed at certain aspect angles (b).

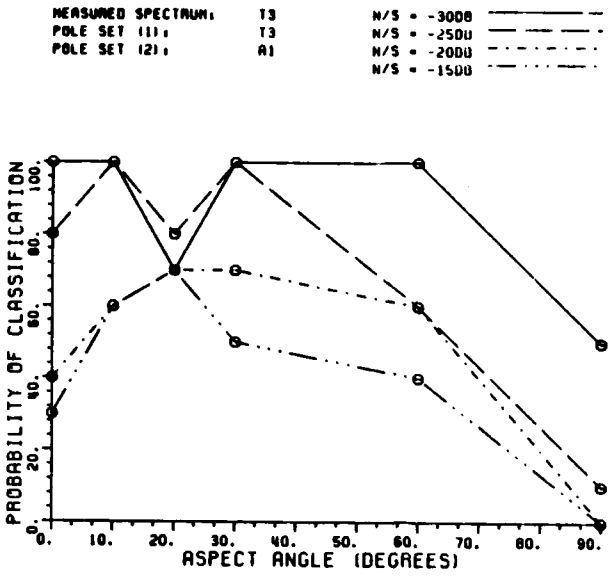

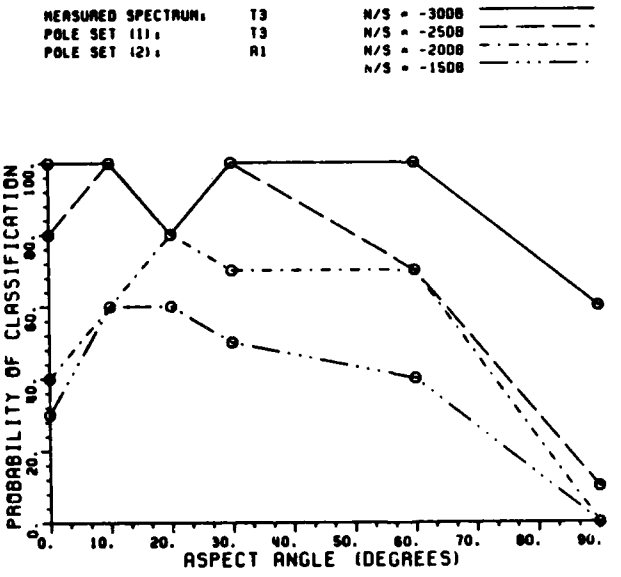

Figure B.11 Probability of classification versus aspect angle for the spectrum of target T3 versus the poles of T3 and A1. Standard case (a), case with some poles removed at certain aspect angles (b).

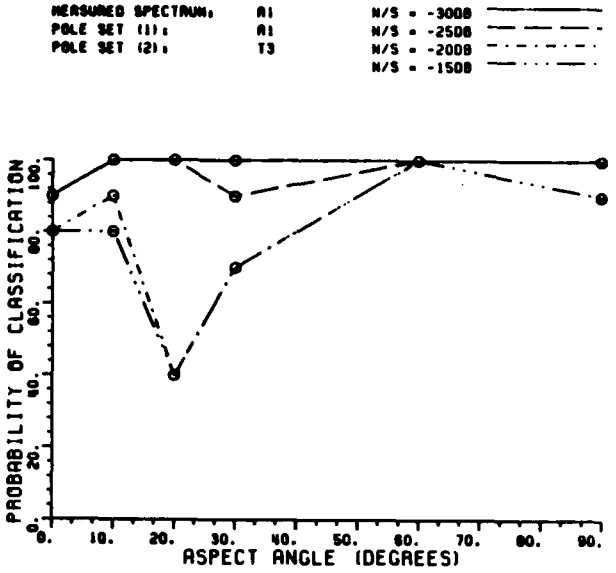

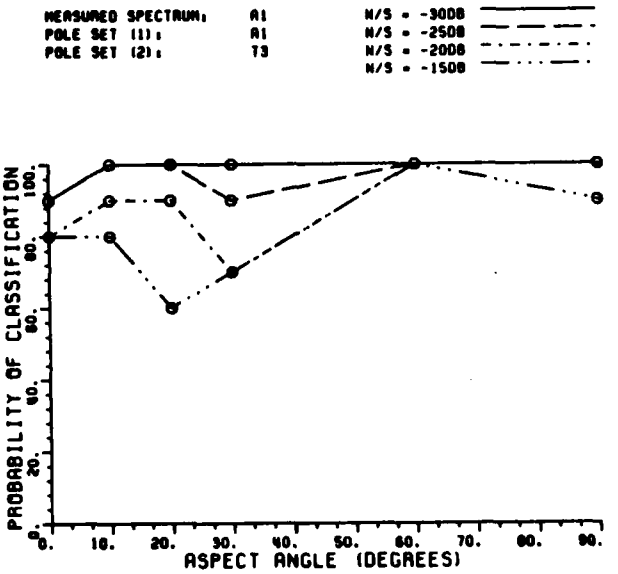

Figure B.12 Probability of classification versus aspect angle for the spectrum of target A1 versus the poles of A1 and T3. Standard case (a), case with some poles removed at certain aspect angles (b).

REFERENCES

[1] E.K. Walton and J.D. Young, "The Ohio State University Compact Radar Cross-Section Measurement Range", IEEE Trans. Antennas and Propagation, Vol. AP-32 No. 11, pp. 1218-1223, Nov. 1984.

[2] D.L. Moffatt, J.D. Young, E.K. Walton and W.L. Leeper, "Resonant Structure NCTR," Final Report No. 714190-2, The Ohio State University Electroscience Laboratory, Department of Electrical Engineering, Columbus, Ohio, January 1983.

[3] M.A. Morgan, "Singularity Expansion Representations of Fields and Currents in Transient Scattering", IEEE Transactions on Antennas and Propagation, Vol. AP-32, No. 5, May 1984.

[4] L.W. Pearson, "A Note on the Representation of Fields as a Singularity Expansion", IEEE Transactions on Antennas and Propagation, Vol. AP-32, No. 5, May 1984.

[5] E.M. Kennuagh, R.L. Cosgriff," The Use of Impulse Response in Electromagnetic Scattering Problems", 1958 IRE Nat'l. Conv. Rec., Pt.1, pp. 72-77 1958.

[6] E.M. Kennuagh, D.L. Moffatt," Transient and Impulse Response Approximations", Proc. IEEE, Vol. 53, pp. 893-901, August 1965.

[7] D.J. Burr and Y.T. Lo," Remote Sensing of Complex Permitivity by Multipole Resonances in RCS", IEEE Transactions on Antennas and Propagation, Vol. AP-21, No.4, pp. 554-561, July 1973.

[8] J.A. Stratton, Electromagnetic Theory, McGraw-Hill Book Co., New York, New York, 1941 .

[9] L. Page, N. Adams, Electrodynamics, Dover Publications, New York, New York, 1940.

[10] T.C. Lee, "Approximate Methods for obtaining the Complex Natural Electromagnetic Oscillations of an object", Dissertation, The Ohio State University, Department of Electrical Engineering Columbus, Ohio, 1983.

[11] L.B. Felsen, "Comments on Early Time SEM", IEEE Trans. Antennas and Propagation, Vol. AP-33 (1), January 1985, pp. 118-120.

[12] M.L. Van Blaricum and R. Mittra, "A Technique for Extracting the Poles and Residues of a System Directly from its Transient Response", IEEE Transactions on Antennas and Propagation, Vol. AP-23, No.6, November 1975.

[13] R. Prony, "Essai Experimental et Analytique sur les lois de la Dilatabilite de Fluide Elastique et sur Celles de la force Expansive de la Vapeur de l'Alkool, a Differentes Temperatures" .J.l' Ecole Polytechnique (Paris), Vol. 1, No. 2 pp 24-76, 1795.

[14] J.N. Brittingham, E.K. Miller, J.L. Willows,"Pole Extraction from Real-frequency Information", Proc. IEEE, Vol. 68, No. 2, pp. 263-273 February, 1980.

[15] N. Chamberlin, "Surface Ship Classification Using Multipolarization, Multifrequency Sky-wave Resonance Radar", Masters Thesis, The Ohio State University, Dept. of Electrical Engineering, Cols., Ohio, September 1984.

[15] E.K. Walton and J.D. Young, "Surface ship Target classification Using HF Multifrequency Radar", Final Report 712352-1. The Ohio State University, ElectroScience Laboratory, Columbus, Ohio, May 1980.

[16] R.K. Mains, D.L. Moffatt, "Complex Natural Resonances of an object in Detection and Discrimination", an ElectroScience Laboratory Technical Report (3424-1), The Ohio State University, Department of Electrical Engineering, Columbus, Ohio, June 1974.

[17] F.J. Harris," On the use of Windows for Harmonic Analysis with the Discrete Transform", Proceedings of IEEE, Vol.66, No.1, Jan. 1978.

[18] W.D. Stanley, G.R. Dougherty and R. Dougherty, Digital Signal Processing, Reston Publishing Company Inc., A Prentice Hall Company Reston, Viginia, 1984.

[19] D.L. Moffatt, J.D. Young, A.A. Ksienski, et al." Transient Response Characteristics in Identification and Imaging", IEEE Trans. APS, Vol. AP-29, No. 2, March 1981.

[20] A. Jalloul, "Discrimination of Radar Targets Using Target Complex Natural Resonances", Masters Thesis, The Ohio State University, Dept. of Electrical Engineering, Cols., Ohio, May, 1985.

[21] I. Barrodale and C. Phillips, "Solution of an Overdetermined System of Linear Equations in the Chebyshev Norm", Acm Trans. Math. Software, Vol. 1, No. 3, pp. 264-270, Sept. 1975.

[22] D.L. Moffatt and C.Y. Lai, "Natural Reasonance Estimation", to appear in IEEE Trans. Instrumentation and Measurements.

END

DATE

FILMED

5-88

DTIC